THAMIRYS ANDRADE LOPES

EFEITO DA MODIFICAÇÃO SUPERFICIAL COM DESCARGA DE CORONA EM FILMES DE NANOFIBRA DE PINUS E EUCALIPTO

LAVRAS – MG
2018

THAMIRYS ANDRADE LOPES

EFEITO DA MODIFICAÇÃO SUPERFICIAL COM DESCARGA DE CORONA EM FILMES DE NANOFIBRA DE PINUS E EUCALIPTO

Dissertação apresentada à Universidade Federal de Lavras, como parte das exigências do Programa de Pós-Graduação em Engenharia de Biomateriais, área de concentração em Compósitos e Nanocompósitos Lignocelulósicos, para a obtenção do título de Mestre.

Prof. Dr. Lourival Marin Mendes
Orientador

Profa. Dra. Lina Bufalino
Coorientadora

LAVRAS – MG
2018

Ficha catalográfica elaborada pelo Sistema de Geração de Ficha Catalográfica da Biblioteca Universitária da UFLA, com dados informados pelo(a) próprio(a) autor(a).

Lopes, Thamirys Andrade.

Efeito da modificação superficial com descarga de corona em filmes de nanofibra de pinus e eucalipto / Thamirys Andrade Lopes. - 2018.

79 p. : il.

Orientador(a): Lourival Marin Mendes.

Coorientador(a): Lina Bufalino.

Dissertação (mestrado acadêmico) - Universidade Federal de Lavras, 2018.

Bibliografia.

1. polpas de celulose branqueadas. 2. permeabilidade ao vapor de água. 3. energia de superfície. I. Mendes, Lourival Marin. II. Bufalino, Lina. III. Título.

THAMIRYS ANDRADE LOPES

EFEITO DA MODIFICAÇÃO SUPERFICIAL COM DESCARGA DE CORONA EM FILMES DE NANOFIBRA DE PINUS E EUCALIPTO

THE EFFECT OF SURFACE MODIFICATION WITH CORONA DISCHARGE IN PINUS AND EUCALYPTUS NANOFIBRIL FILMS

Dissertação apresentada à Universidade Federal de Lavras, como parte das exigências do Programa de Pós-Graduação em Engenharia de Biomateriais, área de concentração em Compósitos e Nanocompósitos Lignocelulósicos, para a obtenção do título de Mestre.

APROVADA em 20 de fevereiro de 2018.

Dr. Fábio Akira Mori UFLA

Dra. Margarete Marin Lordelo Volpato EPAMIG

Prof. Dr. Lourival Marin Mendes
Orientador

LAVRAS – MG
2018

A minha avó Maria José, pelo carinho e apoio e por ser meu maior exemplo de vida.

DEDICO

AGRADECIMENTOS

Primeiramente, agradeço a Deus pelos dons da sabedoria, fé, paciência e discernimento que foram de suma importância, durante esses anos, para que eu pudesse chegar até aqui.

À minha família, em especial aos meus pais, José Maria e Marlúcia, pelo apoio incondicional durante essa jornada, nunca me deixando desistir diante dos obstáculos, mesmo estando longe. À minha irmã, Thaynara, pela paciência e companheirismo de sempre, me incentivando e me ajudando, todos os dias, a realizar meu sonho.

À Universidade Federal de Lavras (UFLA), em especial ao Programa de Pós-Graduação em Engenharia de Biomateriais, juntamente com seus professores, por terem me proporcionado a oportunidade de aprendizado, crescimento pessoal e profissional.

À Coordenação de Aperfeiçoamento de Pessoal de Nível Superior (CAPES), pela concessão da bolsa de mestrado.

Ao professor Lourival Marin Mendes e à professora Lina Bufalino, pela orientação, amizade, carinho, exemplo profissionais e pela confiança por todos esses anos de trabalho juntos.

À Unidade Experimental em Painéis de Madeira (UEPAM) e ao Laboratório de Nanotecnologia, pela estrutura disponível, essencial para a realização do meu projeto.

Ao Núcleo de Estudos em Painéis de Madeira (NEPAM), juntamente com seus membros, que estavam sempre prontos para me ensinar e me auxiliar.

Ao Sr. Arley, técnico da UEPAM, por todo serviço prestado e à Viviane, querida Vivi, pelas prosas e seu cafezinho delicioso de cada dia.

À turma do povo do Miau (Carlos, Aline, Marcelinho, Pri, Maycon, Vica, Maraí, Ariane, Adilson, Bruno, Rosi, Thiago, Ana Luiza e Lipe) e à turma

da quinta série (Luana, Matheus, Uasmin, Mário, Luiz, Luiza, Maryella, Lays e Maressa), por dividirem alegrias e tristezas, dificuldades e vitórias comigo, durante essa jornada.

Às pessoas com quem morei, por fazerem meus dias mais felizes.

Às amizades que fiz em Lavras, que sempre confiaram em mim e sempre me impulsionaram, me fazendo sempre acreditar que eu era capaz de vencer, e a todos que, mesmo indiretamente, torceram e me ajudaram a realizar meu sonho.

RESUMO

Estudos demonstraram que o tratamento corona é promissor para a melhoria da qualidade de tecidos e compósitos. Não há relatos sobre a sua eficácia para a modificação superficial de filmes de nanofibras para impressão e embalagem. Este estudo foi realizado com o objetivo de avaliar as propriedades do filme com a evolução da exposição à descarga corona em filmes de nanofibras de eucalipto e pinus. As nanofibras de celulose foram produzidas a partir de polpas comerciais de celulose branqueadas de ambas as espécies, por meio de 30 passagens em um moinho SuperMasscolloiderGrinder. Os filmes foram obtidos pelo método *casting*. A descarga corona foi aplicada durante 10, 30, 60 e 300 segundos, a uma distância de 3 cm. Além disso, a duração da modificação da superfície foi avaliada após 6, 24, 48, 72 e 96 horas. A descarga corona promoveu a formação de grupos hidroxila, carbonila e outros grupos funcionais pela quebra de ligações C-C e subsequente reação com oxigênio. O melhor tempo de tratamento corona foi de 30 segundos, para o qual foi encontrada máxima permeabilidade ao vapor de água de 13,1 g.mm/KPa.day.m² e 14,2 g.mm/KPa.day.m², para os filmes de eucalipto e pinus, respectivamente. Além disso, observou-se máxima absorção de água (cerca de 35%) para filmes de ambas as espécies tratadas por 30 segundos. A força de tração aumentou com maior tempo de exposição ao tratamento corona. Os filmes de nanofibras de pinus tiveram desempenho melhor que os filmes de nanofibras de eucalipto, devido ao maior índice de cristalinidade e dimensões de nanofibras. Por meio da análise do ângulo de contato e da energia da superfície, verificou-se que a impressão de filmes de nanofibrilas tratados com corona deve ser realizada em até 24 horas, quando os filmes ainda exibem o efeito do tratamento.

Palavras-chave: Polpas de celulose branqueadas. Permeabilidade ao vapor de água. Energia de superfície. Durabilidade.

ABSTRACT

Investigations have shown that corona treatment is promising for quality improvement of fabrics and composites. There are no reports on its effectiveness for surface modification of nanofibril films for printing and packaging purposes. This investigation aimed to evaluate the film properties with the evolution of corona discharge exposition on eucalyptus and pinusnanofibril films. Cellulose nanofibrilswere produced from commercial bleached cellulose pulps of both species through 30 passages in a SuperMasscolloider Grinder. Films were formed by casting method. The corona discharge treatment was applied for 10, 30, 60 and 300 s, at a distance of 3 cm. Furthermore, the duration of the surface modification was evaluated after 6, 24, 48, 72 and 96 h. Corona discharge promoted formation of hydroxyl, carbonyl and other functional groups by the breakage of C-C bonds and subsequent reaction with oxygen. The best corona treatment time was 30 s, for which maximum water vapor permeability of 13.1 g.mm/KPa.day.m² and 14.2 g.mm/KPa.day.m² was found for the eucalyptus and pinus films, respectively. In addition, maximum water absorption (of around 35%) was observed for films of both species treated for 30 s. The tensile strength increased by increasing corona treatment exposition. Pinusnanofibril films showed better performance than eucalyptus nanofibril films due to higher crystalline index and nanofibril dimensions. Through the analysis of contact angle and surface energy, it was verified that printing of corona treated nanofibril films should be carried out up to 24 h where the films still exhibit the effect of the treatment.

Key-words: Bleached cellulose pulps. Water vapor permeability. Surface energy. Durability.

LISTA DE FIGURAS

PRIMEIRA PARTE

SEGUNDA PARTE

LISTA DE TABELAS

PRIMEIRA PARTE

SEGUNDA PARTE - ARTIGO

SUMÁRIO

PRIMEIRA PARTE

1 INTRODUÇÃO

A nanotecnologia é um campo da ciência que apresenta rápida expansão e influencia significativamente outras áreas, tais como medicina, farmácia e a indústria alimentícia, de cosméticos e de embalagens, algumas com vários produtos já disponíveis para comercialização.

Dessa forma, o interesse pela produção e a aplicação de nanofibras de celulose se manteve crescente nos últimos anos (SIRÓ; PLACKETT, 2010). Características como baixa densidade e expansão térmica, abundância, biodegradabilidade e caráter renovável, combinadas com alta resistência e rigidez, as tornam um material interessante para reforçar diferentes matrizes poliméricas e produzir filmes nanocelulósicos (GONZÁLEZ el al., 2014).

Além desses fatores, a utilização de fibras naturais vem aumentando, devido ao menor custo e menor dano ambiental, quando comparadas às fibras sintéticas, sendo empregadas na indústria de materiais, na construção civil e na indústria automobilística e aeronáutica (MARTINS; MATTOSO; PESSOA, 2009).

Os filmes ou compósitos que contêm nanofibras de celulose apresentam melhor resistência mecânica e propriedades de barreira devido à capacidade das nanofibras de celulose de formar redes por meio de ligações de hidrogênio, além de serem biodegradáveis (LEE et al., 2011; BORGES et al., 2010).

As nanofibras de celulose são obtidas por meio da desintegração de matéria-prima lignocelulósica, em que a madeira é, certamente, o recurso mais explorado para essa finalidade (BUFALINO, 2014).

Para se obter filmes de nanofibras de celulose com uma superfície mais reativa, podem ser realizados tratamentos químicos e físicos. Dentre as

possibilidades, pode-se destacar a descarga corona, pela qual se ativa a oxidação superficial das fibras celulósicas, mudando sua energia (BELGACEM et al., 1994).

Alguns estudos foram realizados sobre a aplicação da descarga corona para a modificação superficial da fibra de juta utilizada em compósitos com resina epóxi (GASSAN; GUTOWSKI, 2000) e de pinus, eucalipto e bagaço de cana-de-açúcar, utilizados em compósitos com poliéster (MESQUITA et al., 2017). Esses estudos foram realizados com o objetivo de aumentar a adesão entre fibra e matriz. Além disso, Carvalho, Giordano e Campos (2012) aplicaram a descarga corona em tecido de algodão para aumentar sua hidrofilicidade. No entanto, não há estudos que relatem a aplicação da descarga corona em filmes de nanofibras.

2 OBJETIVO

Este trabalho foi realizado com o objetivo de avaliar o efeito do tratamento corona em filmes de nanocelulose.

2.1 Objetivos específicos

Especificamente, os objetivos foram os seguintes:

a) avaliar a efetividade da aplicação da descarga corona na modificação da energia de superfície dos filmes de nanofibras de celulose;

b) comparar a influência do tratamento corona na qualidade de filmes de nanofibras de celulose de pinus e eucalipto;

c) determinar a durabilidade do tratamento corona por meio do ensaio de ângulo de contato

3 REVISÃO BIBLIOGRÁFICA

3.1 O pinus e o eucalipto no Brasil

A indústria brasileira de árvores plantadas é, atualmente, referência mundial, devido à sua atuação pautada na sustentabilidade, na competitividade e na inovação. As plantações são destinadas à produção de celulose, papel, painéis de madeira, pisos laminados, carvão vegetal e biomassa (IBÁ, 2017).

Segundo o relatório anual da Indústria Brasileira de Árvores (IBÁ, 2017), a área total de árvores plantadas no Brasil totalizou 7,8 milhões de hectares, em 2015, um crescimento de 0,8% em relação ao ano de 2014. Os plantios de pinus ocupam 1,6 milhão de hectares e concentram-se nos estados do Paraná (42%) e de Santa Catarina (34%). Já os plantios de eucalipto ocupam 5,6 milhões de hectares da área de árvores plantadas do país e estão localizados, principalmente, em Minas Gerais (24%), em São Paulo (17%) e no Mato Grosso do Sul (15%).

Da área total de arvores plantadas no Brasil em 2016, 34% pertencem às empresas do segmento de celulose e papel, o que viabiliza o uso dessas espécies para a obtenção de nanofibras de celulose.

3.2 Fibras lignocelulósicas

As fibras vegetais podem ser retiradas de diferentes partes da planta, como caule (juta, malva, bagaço de cana-de-açúcar, bambu), folha (sisal, bananeira, abacaxi, curauá), fruto (aldodão, coco, açaí), tronco (madeira) e outros.

O campo de emprego dessas fibras é bastante amplo, abrangendo aplicações clássicas na indústria têxtil, na indústria moveleira (MDF) e de papel

e celulose, também como reforço em matrizes poliméricas termoplásticas e termofixas e, mais recentemente, como materiais absorventes de metais pesados no tratamento de resíduos industriais, entre outras aplicações (MARINELLI et al., 2008).

As fibras destinadas às aplicações citadas são, geralmente, oriundas de plantios comerciais de pinus, que pertencem ao grupo das coníferas, e de eucalipto, que pertence ao grupo das folhosas.

Conforme se observa na Figura 1, em termos estruturais, as madeiras de coníferas são relativamente simples, sendo compostas quase que totalmente por um único tipo de células alongadas (2 a 5 mm) denominadas traqueídeos longitudinais. Células transversais que compõem o raio e os canais de resina também ocorrem em menor proporção. As madeiras de folhosas, por sua vez, são estruturalmente mais complexas e apresentam maior diversidade de padrões de organização celular. Três tipos principais de células são encontradas neste grupo vegetal, os elementos de vaso, as fibras e as células do raio, que constituem o parênquima radial. Os elementos de vasos (0,2 a 0,5 mm de comprimento) e as fibras (1,0 a 2,0 mm de comprimento) ocorrem em maior quantidade (CARVALHO et al., 2009).

Figura 1Micrografia da seção tangencial da madeira de conífera (A) e de folhosa (B).

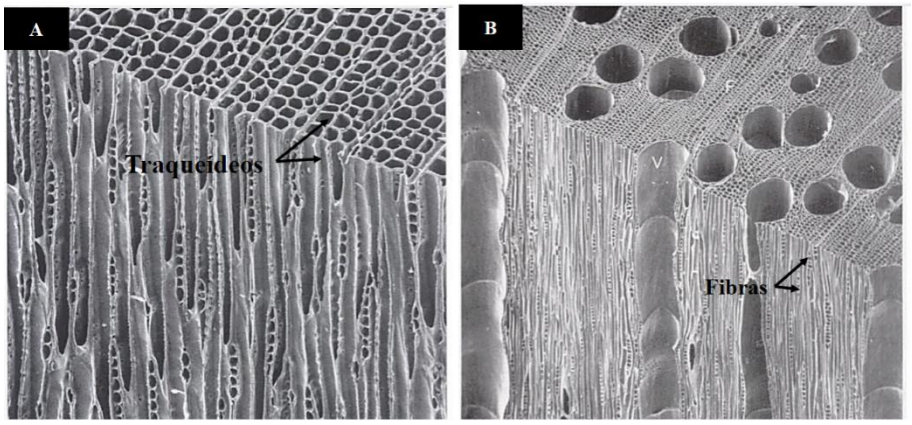

Fonte: BARNETT; JERONIMIDIS (2003)

Na célula vegetal (Figura 2), a parede celular primária típica é composta de microfibrilas de celulose (9% a 25%), uma matriz de hemiceluloses (25% a 50%) e pectinas (10% a 35%). Já a parede celular secundária contém celulose (40% a 80%) na forma de macrofibrilas, hemiceluloses (10% a 40%) e lignina (5% a 25%) (BHATNAGAR; SAIN, 2005).

Figura 2 – Representação esquemática de uma célula vegetal: lamela média (LM); parede primária (P); parede secundária externa (S1); parede secundária média (S2); parede secundária interna (S3); lúmen (L).

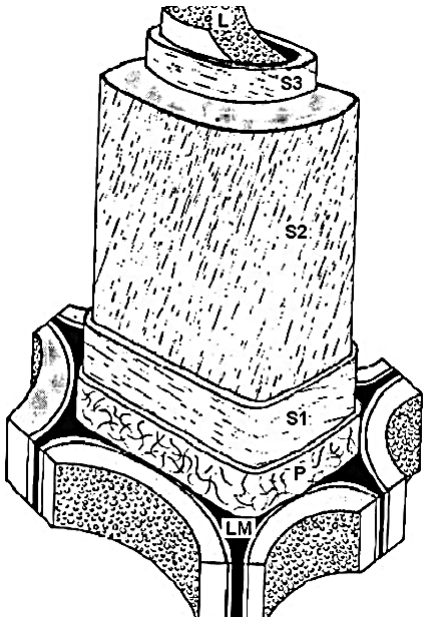

Fonte: Adaptado de Fengel e Wegener (1989)

A organização e a orientação das macrofibrilas nas diferentes camadas da parede celular conferem às fibras e aos traqueídeos longitudinais resistências mecânicas diferentes, o que é relevante para os processos de tratamento, como o cozimento, o refino e o branqueamento. Dentre estas camadas, destaca-se a intermédia S2 da parede secundária, por ter maior espessura e apresentar as estruturas macrofibrilares com orientação aproximadamente paralela ao eixo da fibra (CHINGA-CARRASCO, 2011).

Nas fibras de espécies madeireiras, como é o caso do pinus e do eucalipto, o cozimento kraft e o branqueamento da polpa celulósica promovem a retirada de mais da metade das hemiceluloses e quase a totalidade da lignina por dissolução. A celulose, apesar de ficar parcialmente degradada com estes

processos, não se dissolve. O teor de hemiceluloses na pasta inicial é uma característica importante, na medida em que, quanto maior a percentagem de hemiceluloses, maior será o número de ligações entre as fibras, tornando a polpa menos porosa e mais resistente (NUNES, 2014).

Quanto à presença de hemiceluloses, Iwamoto, Abe e Yano (2008) citam que elas podem facilitar a obtenção de nanofibrilas durante o tratamento mecânico da polpa e aumentam as propriedades físicas de nanocompósitos. No processo de secagem, a presença de hemiceluloses impede a formação de ligações de hidrogênio irreversíveis entre as microfibrilas.

Quanto à lignina, situada na lamela média, se ela não for removida, vai também dificultar o acesso dos reagentes à fibra. Todos estes aspectos influenciam a aptidão de fibrilação das fibras, bem como os diferentes métodos de extração das nanofibras de celulose (DUCHESNE et al., 2001).

3.3 Nanofibras de celulose

As nanofibras de celulose são obtidas da celulose, a qual é encontrada em materiais lignocelulósicos ou pode ser sintetizada por algumas algas, bactérias ou tunicatos (HULT; LARSSON; IVERSEN, 2000).

A celulose é um homopolissacarídeo linear constituído por moléculas de glucose unidas entre si por meio de ligações glicosídicas do tipo β (1→4) (Figura 3), que resultam da perda de uma molécula de água. Apresenta estrutura fibrilar e é envolvida por uma matriz de lignina e hemiceluloses, com módulo de elasticidade alto (FENGEL; WEGENER, 1989).

Figura 3 – Estrutura química da celulose.

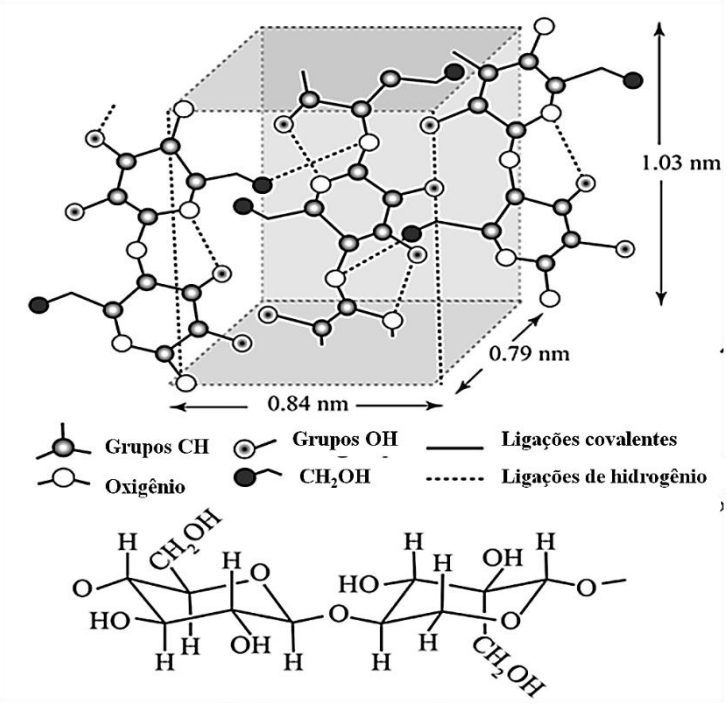

Fonte: Adaptado de Ali e Gibson (2012)

As nanofibras de celulose foram obtidas, pela primeira vez, por Turbak et al. (1983), que utilizaram uma suspensão de fibras de coníferas e fizeram várias passagens dessa suspensão por um homogeneizador de alta pressão, apresentando dimensões laterais em escala nanométrica.

Apresentando diâmetro de 5 a 50 nm e comprimento na ordem de micômetros dependente da fonte (NECHYPORCHUK; BELGACEM; BRAS, 2016), as nanofibras de celulose podem ser consideradas um elemento estrutural importante da celulose.

As nanofibras podem ser obtidas utilizando-se dois processos, sendo eles o “top-down” e o “bottom-up”. No processo “top-down”, as nanofibras são obtidas a partir de macroestruturas reduzidas para atingir a nanoescala. No

processo “bottom-up”, átomos e moléculas se combinam para formar as nanoestruturas (NUNES, 2014) e esses dois processos incluem os métodos mecânicos, químicos e biológicos (Tabela 1).

Tabela 1 – Métodos de obtenção de nanofibras de celulose.

Bottom-up	Top-down	
Bacteriana	Homogeneização	Explosão a vapor
	Moagem	Moinho de bolas
Tunicatos	Refinamento	Hidrólise enzimática
	Extrusão	Carboxilação via TEMPO
Electrospinning	*Blending*	Carboxilação via periodato
	Quaternização	Carboximetilação
	Sulfonação	*Cryocrushing*
	Ultrassom	

Fonte: Adaptado de Nechyporchuk; Belgacem; Bras, 2016

3.3.1 Método mecânico para a obtenção de nanofibras

As nanofibras são produzidas em meio aquoso, enfraquecendo as ligações de hidrogênio interfibrilar, facilitando a desfibrilação. Tipicamente, a celulose é dispersa em baixas concentrações (<5% em massa). Devido à sua elevada capacidade de absorção de água, obtêm-se suspensões altamente viscosas, difíceis de manusear, devido à baixa concentração de sólidos (NECHYPORCHUK; BELGACEM; BRAS, 2016).

Os moinhos Super Mass Colloider são comumente utilizados nesse processo, no qual a suspensão celulósica é passada entre dois discos de carbeto de silício. A distância entre esses discos pode ser ajustada para evitar o problema de entupimento. Por forças de cisalhamento promovidas pelos discos, a parede celular é desintegrada e as nanofibrilas são individualizadas.

Taniguchi e Okamura (1998) descreveram a produção de nanofibras utilizando suspensões de fibras vegetais de diferentes fontes naturais com concentração 5% a 10%, passando-as 10 vezes pelo moinho. O resultado foram suspensões de nanofibras com diâmetro entre 20a 90 nm.

Para aumentar a eficiência de desfibrilação, Wang et al. (2012) relataram a redução da distância entre pedras de moagem a 100 μm da posição zero do movimento. A posição de movimento zero é a posição de contato entre duas pedras, antes do carregamento de celulose.

3.4 Filmes de nanofibra de celulose

Os filmes de nanocelulose são definidos como folhas compostas, feitos completamente de nanofibrilas de celulose (YOUSEFI et al., 2013) de alta resistência e são obtidos por procedimentos semelhantes àqueles para a obtenção do papel. (HENRIKSSON et al., 2008; SEHAQUI et al., 2011).

Podem ser produzidos a partir de uma suspensão contendo água e nanofibrilas de celulose, sendo a água evaporada à temperatura ambiente ou em estufa. A suspensão também pode ser previamente filtrada para retirar o excesso de água e assim formar o filme (GONZÁLEZ et al., 2014).

Ainda que a porosidade de filmes nanocelulósicos seja de 28%, eles apesentam uma interessante combinação de módulo de elasticidade (13,2 GPa), resistência à tração (214 MPa) e tensão na ruptura (10%) (HENRIKSSON et al., 2008). São muito utilizados como membrana porosa em células de combustível (LIU et al., 2003), catálise, purificação e filtragem de líquidos (GRYAZNOV, 1999), imobilização e separação de proteínas (YE et al., 2003) e na engenharia de tecidos (JOHNSON; GHOSH; LANNUTTI, 2007).

3.5 Tratamento com descarga corona

A descarga corona usa o ar atmosférico como meio de reação, sendo gerada com uma alta voltagem e potencial excedendo o ponto de ruptura do ar, que é da ordem de 26 KV/cm (ALMEIDA, 2006). Como resultado, são gerados radicais que iniciam reações de oxidação modificando o material. Esses radicais reagem com o oxigênio, grupos hidroxilas e água, causando mudança apenas nas propriedades superficiais (STEPCZYÑSKAL, 2015).

Esse tratamento é realizado em polímeros para modificar sua superfície. A descarga é gerada a partir de uma diferença de potencial elétrica aplicada entre a ponta e o plano do equipamento. Ao redor da extremidade da ponta, a qual apresenta uma região de elevado campo elétrico, a descarga corona aparece como uma luminescência de cor azul-clara e os elétrons gerados interagem com as moléculas gasosas, originando espécies ativas, tais como íons, radicais e moléculas excitadas. Estas espécies ativas são depositadas na superfície do material, podendo causar modificações nas suas propriedades de superfície (SCHUTZE et al., 1998).

A placa plana, geralmente, é coberta com um material isolante para prevenir a formação de arco voltaico entre os eletrodos. Os parâmetros que influenciam as propriedades superficiais do polímero tratado são potência empregada, distância ponta-plano, umidade relativa e temperatura (CHAN, 1994).

O tratamento corona é uma tecnologia utilizada frequentemente pela indústria de embalagens para aumentar a tensão superficial e a polaridade de filmes, a fim de melhorar a capacidade de impressão, a molhabilidade e as propriedades de adesão. O tratamento consiste em gerar uma descarga elétrica visível de uma disposição linear de eletrodos sobre a superfície do polímero ao aplicar baixa voltagem (10 a 40 kV) em alta frequência (1-4 kHz). A descarga

corona provoca ionização parcial da atmosfera circundante e produz espécies excitadas (por exemplo, radicais livres, íons ou elétrons). Essas espécies químicas são capazes de reagir e de oxidar as moléculas expostas à superfície do polímero, formando novas funcionalidades polares, tais como grupos hidroxilo, carboxilo, carbonilo e amida na superfície. As novas funcionalidades resultantes têm forte compatibilidade com materiais hidrofílicos e aumentam a adesão com camadas finas como revestimentos, vernizes, adesivos, membranas (KUREK; DEBEAUFORT, 2015).

Outro efeito bem conhecido dessa ionização parcial da atmosfera é uma nanomodificação da superfície física do polímero, como consequência de um fenômeno de abrasão chamado gravura. O tratamento corona poderia ser, assim, considerado um processo simultâneo de deposição/remoção de espécies químicas sobre superfícies movidas por íons e radicais (PANKAJ et al., 2014).

3.6 Molhabilidade e energia livre de superfície

A hidrofilicidade de uma superfície sólida é geralmente expressa em termos de molhabilidade que pode ser quantificada por medidas de ângulo de contato. O valor do ângulo de contato (θ) pode variar de 0 a 180°. Quando θ for igual a zero, indica que o líquido molha completamente a superfície sólida e espalha-se livremente sobre esta à uma taxa dependente da viscosidade do líquido e da rugosidade da superfície. Quando o ângulo de contato for maior que zero e menor que 180°, o líquido molha parcialmente a superfície do sólido. No caso onde o ângulo de contato é igual a 180°, o molhamento da superfície é praticamente desprezível, sendo considerado como nulo. Desta forma, a tendência para um líquido se espalhar ou molhar a superfície de um sólido aumenta quando o ângulo de contato diminui (CHAN 1994).

Este ângulo de contato pode ser medido utilizando-se a técnica da gota séssil em que a quantificação pode ser feita colocando-se uma gota de um líquido sobre uma superfície sólida podendo ser observado dois fenômenos: o líquido se espalha inteiramente sobre a superfície, ou permanece na forma de gota estabelecendo um ângulo de contato definido entre a fase líquida e a fase sólida (CARVALHO, 2009).

No caso de líquidos, a energia livre superficial pode ser definida como uma força atuando paralelamente à superfície por unidade de comprimento. Porém, no caso dos sólidos, as moléculas que atuam na superfície não são equivalentes e a velocidade com que elas podem se arranjar de maneira a se tornarem equivalentes é pequena. Não há métodos diretos para medição de energia livre ou tensão superficial de sólidos. Entretanto, existem vários métodos indiretos empíricos e semi-empíricos baseados na medição de ângulo de contato (CHAN, 1994).

REFERÊNCIAS

ALI, Z. M.; GIBSON, L. J. The structure and mechanics of nanofibrillar cellulose foams. **Soft Matter**, LesUlis, v. 9, n. 5, p. 1580-1588, 2012.

ALMEIDA, E. C. **O tratamento corona em filmes e peças plásticas**. 2006. Disponível em: <http://www.coronabrasil.com.br/tratamento-filmes-pecas plasticas.html>. Acesso em: 18 dez. 2017.

BARNETT, J. R.; JERONIMIDIS, G. **Wood quality and its biological basis**. Hoboken: Blackwell, 2003.

BELGACEM, M. N. et al. Effects of corona modification on the mechanical properties of polypropylene cellulose composites. **Journal of Applied Polymer Science**, New York, v. 53, p. 379-385, 1994.

BHTNAGAR, A.; SAIN, M. Processing of cellulose nanofiber-reinforced composites. **Journal of Reinforced Plastics and Composites**, Westport, v. 24, n. 12, p. 1259-1268, 2005.

BORGES, A. C. et al. Curing kinetics and mechanical properties of a composite hydrogel for the replacement of the nucleus pulposus. **Composites Science and Technology**, Barking, v. 70, p. 1847-1853, 2010.

BUFALINO, L. **Filmes de nanocelulose a partir de resíduos madeireiros da Amazônia**. 2014. 106 p. Tese (Doutorado em Ciência e Tecnologia da Madeira)-Universidade Federal de Lavras, Lavras, 2014.

CARVALHO, J. G.; GIORDANO, J. B.; CAMPOS, J. S. C. Medidas quantitativas de absorção de água em tecidos de algodão e poliéster antes e após trtamento corona. **Química Têxtil**, São Paulo, v. 108, p. 58-67, 2012.

CARVALHO, W. et al. Uma visão sobre a estrutura, composição e biodegradação da madeira. **Química Nova**, São Paulo, v. 32, n. 8, p. 1-5, 2009.

CHAN, C. M. **Polymer surface modification and characterization**. Munich: Hanser; Gardner, 1994. 285 p.

CHINGA-CARRASCO, G. Cellulose fibres, nanofibrils and microfibrils: the morphological sequence of MFC components from a plant physiology and fibre technology point of view. **Nanoscale Research Letters**, London, v. 6, n. 1, p. 417-424, 2011.

DUCHESNE, I. et al. The influence of hemicellulose on fibril aggregation of kraft pulp fibres as revealed by FE-SEM and CP/MAS 13C-NMR. **Cellulose**, Bucharest, v. 8, n. 2, p. 103-111, 2001.

FENGEL, D.; WEGENER, G. **Wood:** chemistry, ultrastructure, reactions. Berlin: W. de Gruyter, 1989.

GASSAN, J.; GUTOWSKI, V. S. Effects of corona discharge and UV treatment on the properties of jute-fbre epoxy composites. **Composites Science and Technology**, Barking, v. 60, p. 2857-2863, 2000.

GONZÁLEZ, I. et al. From paper to nanopaper: evolution of mechanical and physical properties. **Cellulose**, Bucharest, v. 21, n. 4, p. 2599-2609, 2014.

GRYAZNOV, V. Membrane catalysis. **Catalysis Today**, Amsterdam, v. 51, n. 3, p. 391-395, 1999.

HENRIKSSON, M. et al. Cellulose nanopaper structures of high toughness. **Biomacromolecules**, London, v. 9, n. 6, p. 1579-1585, 2008.

HULT, E. L.; LARSSON, P. T.; IVERSEN, T. Comparative CP/MAS 13C-NMR study of cellulose structure in spruce wood and kraft pulp. **Cellulose**, Bucharest, v. 7, n. 1, p. 35-55, 2000.

INSTITUTO BRASILEIRO DE ÁRVORES. **Histórico de desempenho do setor de árvores plantadas**. Disponível em: <http://iba.org/pt/biblioteca-iba/historico-do-desempenho-do-setor>. Aceso em: 27 nov. 2016.

IWAMOTO, S.; ABE, K.; YANO, H. The Effect of hemicelluloses on wood pulp nanofibrillation and nanofiber network characteristics. **Biomacromolecules**, London, v. 9, p. 1022-1026, 2008.

JOHNSON, J.; GHOSH, A.; LANNUTTI, J. Microstructure-property relationships in a tissue-engineering scaffold. **Journal of Applied Polymer Science**, New York, v. 104, n. 5, p. 2919-2927, June 2007.

KUREK, M.; DEBEAUFORT, F. Surface modification of packaging films by coatings with bioactive compounds and biopolymers. In: KONTOMINAS, M. G. (Ed.). **Bioactive packaging of foods:** quality and safety issues. Lancaster: Destech, 2015. p. 119-188.

LEE, S. H.; TERAMOTO, Y.; ENDO, T. Cellulose nanofiber-reinforced polycaprolactone/polypropylene hybrid nanocomposite. **Composites Part A**, Kidlinton, v. 42, p. 151-156, 2011.

LIU, F. et al. Nafion/PTFE composite membranes for fuel cell applications. **Journal of Membrane Science**, Amsterdam, v. 212, n. 1, p. 213-223, 2003.

MARINELLI, A. L. et al. Desenvolvimento de compósitos poliméricos com fibras vegetais naturais da biodiversidade: uma contribuição para a sustentabilidade amazônica. **Polímeros:** Ciência e Tecnologia, São Carlos, v. 18, n. 2, p. 92-99, 2008.

MARTINS, M. A.; MATTOSO, L. H. C.; PESSOA, J. D. C. Comportamento térmico e caracterização morfológica das fibras de mesocarpo e caroço do açaí (Euterpe oleracea Mart.). **Revista Brasileira de Fruticultura**, Jaboticabal, v. 31, n. 4, p. 1150-1157, 2009.

MESQUITA, R. G. de A. et al. Polyester composites reinforced with corona-treated fibers from pine, Eucalyptus and sugarcane bagasse. **Journal of Polymers and the Environment**, London, v. 25, n. 3, p. 800-811, Sept. 2017.

NECHYPORCHUK, O.; BELGACEM, M. N.; BRAS, J. Production of cellulose nanofibrils: a review of recent advances. **Industrial CropsandProducts**, London, v. 93, p. 2-25, 2016.

NUNES, T. F. G. **Produção, caracterização e aplicação de nanofibras de celulose**. 2014. 81 p. Dissertação (Mestrado Integrado em Engenharia Química)- Universidade de Coimbra, Coimbra, 2014.

PANKAJ, S. K. et al. Applications of cold plasma technology in food packaging. **Trends in Food Science & Technology**, Cambridge, v. 35, n. 1, p. 5-17, 2014.

SCHÜTZE, A. et al. The atmospheric-pressure plasma jet: a review and comparison to other plasma sources. **IEEE Transactions on Plasma Science**, New York, v. 26, n. 6, p. 1685-1693, 1998.

SEHAQUI, H. et al. Strong and tough cellulose nanopaper with high specific surface area and porosity. **Biomacromolecules**, London, v. 12, n. 10, p. 3638-3644, 2011.

SIRÓ, I.; PLACKETT, D. Microfibrillated cellulose and new nanocomposite materials: a review. **Cellulose**, Bucharest, v. 17, n. 3, p. 459-494, 2010.

STEPCZYÑSKAL, M. Analysis of the decay of some effects of modification of polylactide surface layers. **Polimery**, Warsaw, v. 60, n. 7/8, p. 462-467, 2015.

TANIGUCHI, T.; OKAMURA, K. New films produced from microfibrillated natural fibres. **Polymer International**, London, v. 47, n. 3, p. 291-294, 1998.

TURBAK, A. F.; SNYDER, F. W.; SANDBERG, K. R. **Microfibrillated cellulose**. ITT Rayonier (Shelton, WA). Patent US n. 4374702, 1 Jan. 1983.

WANG, Q. Q. et al. Morphological development of cellulose fibrils of a bleached eucalyptus pulp by mechanical fibrillation. **Cellulose**, Bucharest, v. 19, n. 5, p. 1631-1643, 2012.

YE, S. H. et al. Antifouling blood purification membrane composed of cellulose acetate and phospholipid polymer. **Biomaterials**, Surrey, v. 24, n. 23, p. 4143-4152, 2003.

YOUSEFI, H. et al. Comparative study of paper and nanopaper properties prepared from bacterial cellulose nanofibers and fibers/ground cellulose nanofibers of canola straw. **Industrial Crops and Products**, London, v. 43, n. 1, p. 732-737, 2013.

SECOND PART – ARTICLE

ARTICLE 1 – THE EFFECT OF SURFACE MODIFICATION WITH CORONA DISCHARGE IN PINUS AND EUCALYPTUS NANOFIBRIL FILMS

(Artigo redigido e submetido de acordo com as normas da revista Surface and Coatings Technology)

ARTICLE 1

THE EFFECT OF SURFACE MODIFICATION WITH CORONA DISCHARGE IN PINUS AND EUCALYPTUS NANOFIBRIL FILMS

Thamirys Andrade Lopes[a*], Lina Bufalino[b], Pedro Ivo Cunha Claro[c], Maria Alice Martins[d], Gustavo Henrique Denzin Tonoli[e], Lourival Marin Mendes[e]

[a] Department of Forestry Science, Federal University of Lavras, Lavras, 37.200-000, MG, Brazil (thamiryscpo@hotmail.com)

[b]Institute of Agricultural Sciences, Rural Federal University of Amazonia, Belém, 66.010-000, PA, Brazil (linabufalino@yahoo.com.br)

[c]Department of Materials Science and Engineering, Federal University of São Carlos, São Carlos, SP 13565-905, Brazil (pedrocunhaclaro@ymail.com)

[d]Laboratory of National Nanotechnology of Agriculture (LNNA), Embrapa Instrumentation Unit, São Carlos, 13.560-970, SP, Brazil (maria-alice.martins@embrapa.br)

[e] Department of Forestry Sciences, Federal University of Lavras, Lavras, 37.200-000, MG, Brazil (gustavotonoli@dcf.ufla.br/lourival@dcf.ufla.br)

*Corresponding author. Tel.: +55 35998194086

E-mail address: thamiryscpo@hotmail.com

ABSTRACT

Investigations have shown that corona treatment is promising for quality improvement of fabrics and composites. There are no reports on its effectiveness for surface modification of nanofibril films for printing and packaging purposes. This investigation aimed to evaluate the film properties with the evolution of corona discharge exposition on eucalyptus and pinusnanofibril films. Cellulose nanofibrils were produced from commercial bleached cellulose pulps of both species through 30 passages in a Super Masscolloider Grinder. Films were formed by casting method. The corona discharge treatment was applied for 10, 30, 60 and 300 s, at a distance of 3 cm. Furthermore, the duration of the surface modification was evaluated after 6, 24, 48, 72 and 96 h. Corona discharge promoted formation of hydroxyl, carbonyl and other functional groups by the breakage of C-C bonds and subsequent reaction with oxygen. The best corona treatment time was 30 s, for which maximum water vapor permeability of 13.1 g.mm/KPa.day.m² and 14.2 g.mm/KPa.day.m² was

found for the eucalyptus and pinus films, respectively. In addition, maximum water absorption (of around 35%) was observed for films of both species treated for 30 s. The tensile strength increased by increasing corona treatment exposition. Pinusnanofibril films showed better performance than eucalyptus nanofibril films due to higher crystalline index and nanofibril dimensions. Through the analysis of contact angle and surface energy, it was verified that printing of corona treated nanofibril films should be carried out up to 24 h where the films still exhibit the effect of the treatment.

Key-words: Bleached cellulose pulps; water vapor permeability; surface energy; durability

1 INTRODUCTON

The use of natural fibers has been increasing due to its lower cost and less environmental damage when compared to synthetic fibers. They are applied to materials used in the civil construction, automobile and aeronautics industries [1].

Cellulose nanofibrilsare obtained through the mechanical disintegration of lignocellulosic raw material, being wood the most exploited resource for this purpose[2]. The cellulose nanofibrils exhibit large specific area, very high elastic modulus, high aspect ratio, low thermal expansion, non-abrasive nature, non-toxic character and ability to act as significant reinforcement at low loading levels. These attractive properties stimulate their application as reinforcing agents in the polymer nanocomposites[3–5].

When the water is vaporized, aqueous nanofibrils suspensions are transformed into films by the network that is formed through interfibrillar hydrogen bonding [6]. They exhibit high mechanical performance and optical transparence, low thermal expansion and suitable oxygen barrier properties[7,8].

The modification of nanofibril films to obtain surfaces that are more reactive could expand nanofibril applications. The corona treatment is an easy to apply and low cost technology that is frequently used by the packaging industry to increase the surface tension and polarity of films in order to improve their printing capacity, wettability and adhesion properties [9,10]. It causes a surface oxidation of the polymer that is activated, changing its surface energy [11].

Some studies have been conducted regarding the application of corona discharge for the surface modification of juta fiber used in epoxy composites[12]; and of pinus, eucalyptus and sugarcane bagasse used in polyester composites[13]. Those studies had the purpose of increasing the adhesion between fiber and matrix. Besides, Carvalho; Giordano; Campos [14] applied corona discharge in cotton fabric in order to increase its hydrophilicity.

However, to the best of our knowledge, there are no studies in the literature that report the application of corona discharge in nanofibril films. Besides raising permeability, it is crucial to determine the maximum time available between the corona treatment duration and film utilization. Therefore, this investigation aimed to evaluate the film

properties with the evolution of corona discharge exposition on eucalyptus and pinusnanofibril films.

2. Material and methods

2.1. Materials

Commercial bleached cellulose pulps from *Eucalyptus* sp. and *Pinus* sp. were provided by Klabin Company, located at Santa Catarina, Otacílio Costa, Brazil. The pulps were produced by the kraft process and followed by bleaching. The eucalyptus pulps have a viscosity of 675 $g.cm^{-3}$ and the pine pulps have a viscosity of 633 $g.cm^{-3}$.

2.2. Characterization of the commercial pulps

Chemical composition of the eucalyptus and pinus pulps was determined in triplicates. Previously, the samples were submitted to extraction using a sequence of toluene-ethanol (5 h), ethanol (4 h), and water (2 h). Lignin content was analyzed according to ABNT NBR 7989 [15]standard. The holocellulose content was obtained by the procedure described by Browning [16]. The cellulose content was determined according to the methodology of Kennedy, Phillips and Williams [17].

The hemicelluloses were quantified by the difference between the holocellulose and cellulose contents.

Scanning electron microscopy (SEM) was performed to evaluate the morphology of the bleached fibers. A JEOL scanning electron microscope, model JSM 6510, with a tungsten filament operating at 15 kV was used to obtain the micrographs. The samples were scattered on double-sided carbon adhesive tapes, previously glued on aluminum sample holders (stubs), and covered with gold.

2.3. Production of the cellulose nanofibrils

Cellulose nanofibrilswere obtained by mechanical defibrillation using a Super MasscolloiderMasuko Sangyo MKCA6-2 defibrillator at 1500 rpm with energy efficiency of 1.0 x 10^4 kWh/ton. Initially, the cellulose pulps were immersed in water at a 1.0 % w/v consistency for a 48 h hydration with the purpose of swelling the fiber cell walls. The gap between the silicon carbide stones in the defibrillator was adjusted to 100 µm[18]. The suspension was passed through the grinder 30 times[19] and the electric current consumed was kept at 6A.

2.4. Characterization of the cellulose nanofibrils

Field emission gun scanning electron microscopy (FEG-SEM) was performed to observe the morphology of nanofibrils after defibrillation. The analysis was carried out in JEOL® miscroscope model JSM 6701F that operated at 2 kV. Two drops of the nanofibrils suspension were deposited in 50 mL of deionized water, which was sonicated at 450 W for 1 min on a tipped Brason® ultrasound. Afterwards, a drop of the homogenized suspension was deposited on a silicon plate. The mean diameter of the nanofibrilswas determined by digital image analysis using the ImageJ 1.48v. Hundred measurements were made for the nanofibrils of each genus.

The crystalline structure of the nanofibrils was analyzed by diffractograms obtained in a diffractometer model XRD 600 (Rigaku ®) operating with 30 kV, 30 mA and Cu-Kα radiation (λ = 1540 Å). The samples were deposited in glass sample port and the scanning was performed at a rate of 2θ/min from 5º to 38º. The crystalline index was calculated using the maximum intensity that was obtained at the main and higher peak of the diffractogram and the minimum intensity located

between the two crystalline peaks by Eq. 1, as suggested by Segal et al.[20].

$$CI = \left(1 - \left(\frac{Iam}{Ic}\right)\right) * 100 \quad (1)$$

Where: *CI* is the crystalline index (%); *Iam* is the minimum intensity obtained between the peaks located at 2θ = 16.5° and at 2θ = 22.6°; and *Ic* is the maximum intensity identity of the main crystalline peak.

2.5. Preparation and corona discharge treatment of the nanofibril films

Films were formed by the casting method.Aliquots of 40 mL of the nanofibril suspension were deposited on 15 cm-diameter acrylic Petri dishes and conditioned at 25 ± 5°C and 60% relative humidity for 5 days until the films were dried. Fifteen films were produced for each genus. The surface and cross-section of eucalyptus and pinusnanofibril films were showed in Fig. 1.

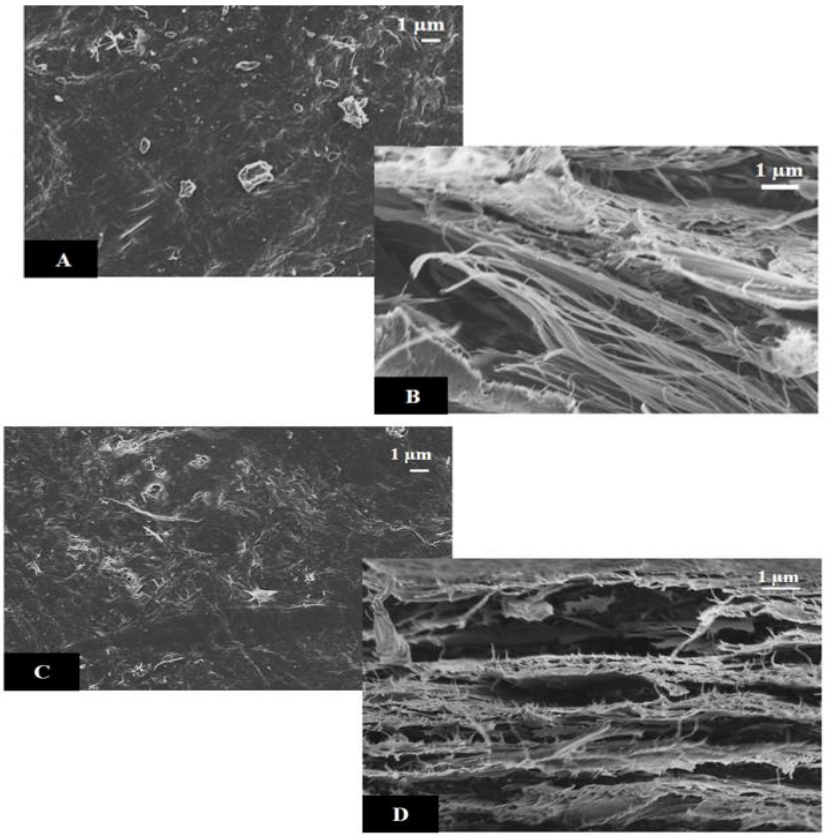

Fig. 1. Aspect of eucalyptus and pinus films. A: surface of eucalyptus film; B: cross-section of eucalyptus film; C: surface of eucalyptus film; D: cross-section of pinus film.

The samples were dried at 60°C for 24 h before corona application. For this, Corona Brasil converter, model PT-1, with power of 0.5 kW was used. The discharge of 10 kV, intensity of 60 µA and frequency of 60 Hzwas applied in dry samples for 10, 30, 60 and 300 s, at

a distance of 3 cm (Fig. 2). The time was controlled using a digital timer. Films without treatment (WT) were evaluated for comparison. Three films were assigned to each treatment.

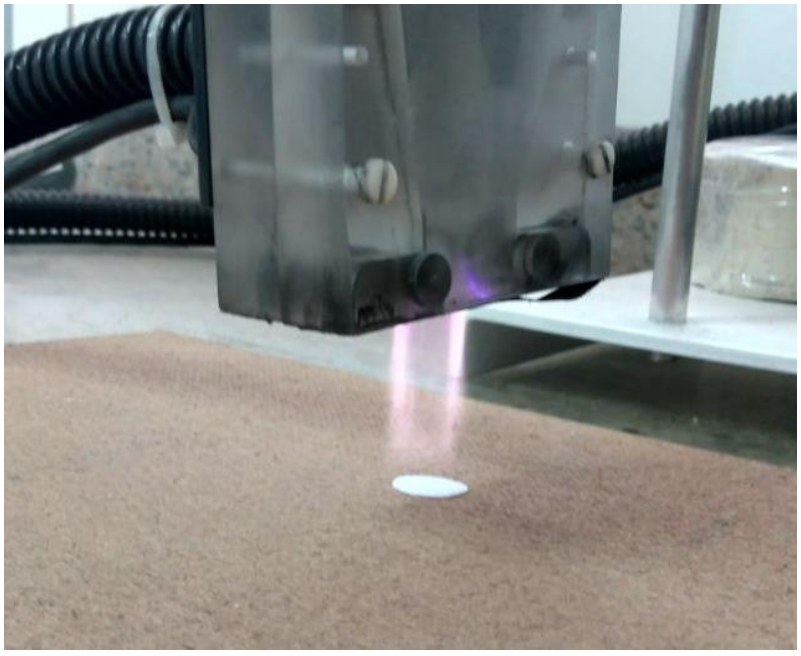

Fig. 2. Application of corona discharge on nanofibril films.

2.6. Characterization of the nanofibril films

A JEOL® microscope model JSM 6701F that operate at 2 kV was used to analyze the surface and cross-section morphology of films. The

samples were scattered on double-sided carbon adhesive tapes, previously glued on aluminum sample holders (stubs), and covered with gold.

The spectra of attenuated total reflectance (ATR) were obtained in a Varian 600-IR Series FT-IR spectrophotometer, equipped with a GladiATR accessory and a diamond tip. The scanning was performed at a 4% resolution and ranged from 4000 cm^{-1} to 400 cm^{-1}, totalizing 32 scans.

The grammage (Eq. 2) values of the nanofibril films were determined before the corona discharge. From each film, two samples were cut to a diameter of 1.6 cm. A balance of 0.0001 g precision was used for weighing. The width and length of samples were determined with a pachymeter with an accuracy of 0.01 mm, while thickness was measured with a micrometer of 0.001 μm precision.

$$Gr = \frac{m}{A} \quad (2)$$

Where: *Gr* is the weight ($g.m^{-2}$); *m* is the mass (g); and *A* is the area (m^2).

The water vapor permeability of the films was determined by gravimetry according to the ASTM E 96-00[21] standard and the literature[22]. For each film, two samples were cut to a diameter of 1.6

cm and placed between the cap and the amber glass vials of the permeability cell with 3/4 of its volume containing silica gel (desiccant), previously oven dried at 150°C for 24 h. Then, the amber glass was placed in hermetic desiccators at 18.5 ± 2°C, whose volume of water sets the water activity in contact with the upper face of the specimen to 0.1. The weight gain was measured every 24 h until 10 days of moisture exposure. The water vapor permeability rate (*WVPR*) of polymer films was estimated using linear regression between weight gain (g) and time (24 h). The slope of the linear part of the curve represents the amount of water vapor diffusion through the specimen per unit time ($g.T^{-1}$). The *WVPR* and the water vapor permeability (*WVP*) were determined by Eq. 3 and 4, respectively:

$$WVPR = \frac{g}{T*A} \quad (3)$$

$$WVP = \frac{WVPR*t}{sp*\frac{Rh}{100} - sp*\frac{Rhi}{100}} \quad (4)$$

Where: *WVPR* is the water vapor permeability rate ($g/h.m^2$); *g/T* is the slope of the line obtained by linear regression of mass gain (g) in

relation to conditioning time (h); *A* is the permeation area of each specimen (m^2); *WVP* is the water vapor permeability ($g.mm/KPa.day.m^2$); *t* is the thickness of the specimen (mm); *sp*is the saturated vapor pressure of the water at the testing temperature of 18.5ºC (KPa); *Rhi* is the relative humidity inside the glass containing white silica gel equals to 0%; and *Rh* is relative humidity inside the desiccator containing distilled water (100%). The *sp* equation was calculated according to equation 5, known as Tetens[23]:

$$sp = 0{,}6108e^{\frac{17{,}27*T}{T+237{,}3}} (5)$$

Where: *sp* is saturated vapor pressure of water at the test temperature of 18.5ºC (KPa); and *T* is the conditioning temperature (18.5ºC) of the desiccator containing cells with biofilms and distilled water.

The water absorption analysis was performed according to Róz[24] at 75% Rh. This condition was achieved with an aqueous sodium nitrite salt solution ($NaNO_2$) according to ASTM E-104[25]. Six samples with 2 cm diameter were cut for each treatment. They were previously dried in an oven at 70°C for 24 h, and subsequently weighed. The

samples were weighed 6 h after the beginning of the test and every 24 h for 5 consecutive days. The amount of water absorbed was expressed as the percentage of the mass gain in relation to the initial mass of the samples according to Eq. 6:

$$WA = \frac{Mc - Mi}{Mi} \quad (6)$$

Where: *WA* is the water absorption (%); *Mc* is the current mass (g); and *Mi* is the dry mass (g).

The maximum tensile strength (σmáx) and the elastic modulus (E) were measured using a TA.XT2i (Stable Micro Systems) texturometer. Tests were performed according to ASTM D 882-09 [26]. The samples dimensions were 10 ± 2 mm of width, 100 ± 10 mm of length and 0.1 ± 0.08 mm of thickness. Five replicates were tested for each time of the corona discharge application. The distance between the jaws, the test velocity and the load cell were 50 mm, 0.8 $mm.s^{-1}$ and 490 N, respectively. The values of the mechanical tensile properties were normalized by the respective grammage (Gr) values of each film.

The wettability and surface free energy determinations was carried out on the films to verify the length or duration of the corona treatment of the films treated for 30 s. This condition was selected as the most effective in the previous stages of the work. The polar and dispersive contribution to surface energy ($mN.m^{-1}$) values of the films were measured by the contact angles formed by distilled water, glycerol and diode-methane solvents. The wettability was obtained by measurement of the contact angle formed by distilled water drops over the films surface. The first measurement was proceeded immediately after the corona treatment (0 h). Further measurements were carried out after 24 h, 48 h, 72 h, 96 h and 120 h. The analysis was conducted using the equipment KRUSS Drop Shape Analyzer, model DSA 25B. The contact angle and surface energy were obtained through Advance software, using the Owens, Wendt, Rabel and Kaelble (OWRK) method.

3. Results and discussion

3.1. Characterization of commercial pulp

The eucalyptus and pinus fibers showed higher percentages of cellulose and lower percentages of hemicelluloses (Table 1).

Table 1. Average and standard-deviation values of the chemical components of the commercial cellulose pulps.

	Cellulose	**Hemicelluloses**	**Lignin**
		Content (%)**	
Eucalyptus	91.9 ± 2.9*	3.0 ± 0.9	Not-detected
Pinus	85.9 ± 1.8	9.9 ± 2.4	Not-detected

* Standad-deviation; ** All values were calculated based on mass free of extractive

Kraft pulping is a chemical process of cellulose production that allows the separation of the wood fibers by the dissolution of the lignin and also are removed the extractives and part of the carbohydrates [27]. Therefore, bleached pulp are suitable for nanofibril production because it contains relatively high cellulose and almost no lignin [28–32]. Lignin may hinder nanofibrillation process through increasing the energy expenditure of the process[33,34]. The removal of lignin increasing the whiteness of the pulp and consequently facilitating the generation of nanofibrils[33,35,36]. For both spices, the amount of lignin was not detected in the analytical analysis.

The presence of hemicelluloses in the cellulosic pulp, because they are hydrophilic, allows greater hydration of the fibers, favoring the defibrillation process of the fibers [37]. They contributes to the adhesion between the nanofibrils in the dry state, leading to the improvement of stiffness and strength of the films [33].

3.2 Characterization of cellulose nanofibrils

The SEM-FEG micrographs (Fig. 3) show the intertwined and disordered networks of cellulose nanofibrils ofeucalyptus and pinus obtained after 30 passages through the defibrillator.

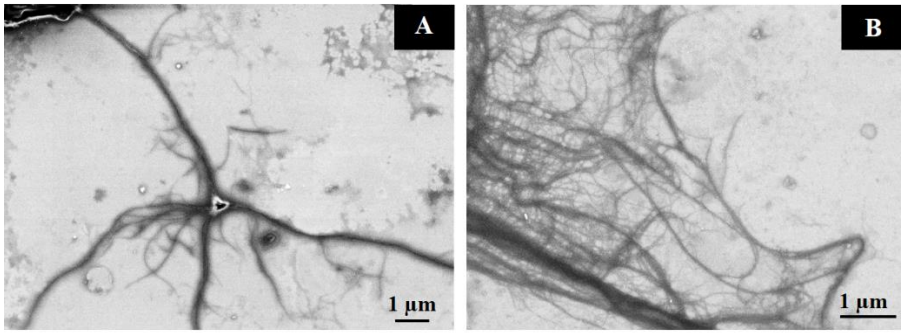

Fig. 3. Typical SEM-FEG micrographs of the eucalyptus (A) and pinus (B) nanofibrils.

The mechanical method to obtain nanofibrils consists of the delaminating the cell wall of the fibers through shear forces generated between discs[38]. Initially, the outer cell layers being the primary layer and the S1 sub layer are disaggregated, which results in the exposure of the S2 layer [39]. Cellulose nanofibrilsare then generatedby shearing and consist mainly of microfibril aggregates that are removed from the surface [40,41].

The type of equipment and parameters defined in the process (such as the speed of rotation, distance between disks, number of cycles in the mill), and fiber type will directly influence the quality of their respective nanofibrils[42,43]. Through Fig. 4 it is possible to observe the average diameters of eucalyptus and pinusnanofibrils.

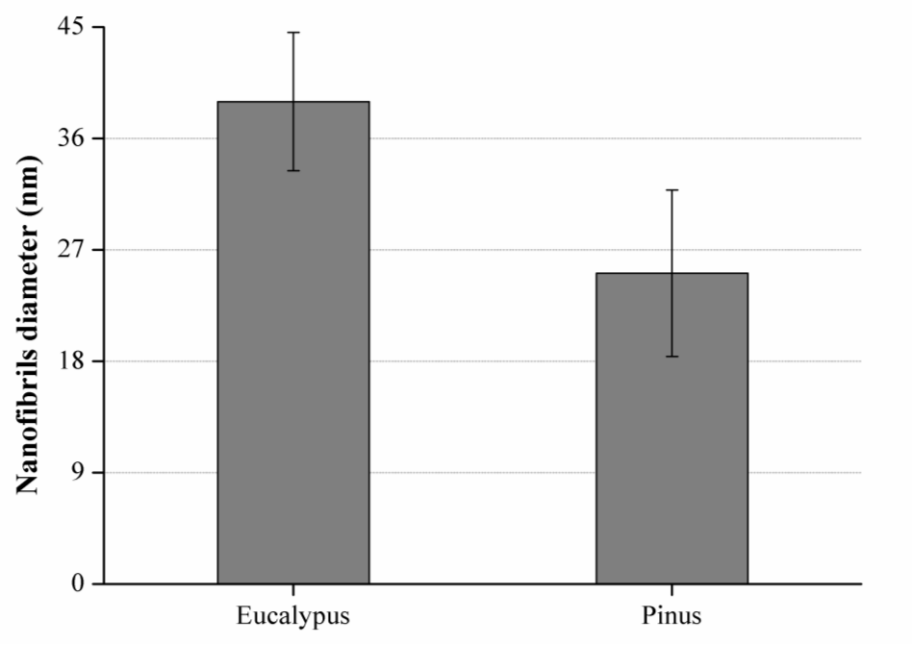

Fig. 4. Average and standard deviation values of the diameters of eucalyptus and pinusnanofibrils

The eucalyptus and pinusnanofibrils had an average diameter of 39 nm and 25 nm, respectively. The average diameter values obtained for nanofibrils are below this value.

The length of the nanofibrils is difficult to evaluate due to its excessive interlacing, although it is known that it is of the order of a few millimeters. Thus, nanofibrils obtained by mechanical process generally present high aspect ratio[43].

In structural terms the coniferous woods are relatively simple, being composed almost entirely by a single type of elongated cells called tracheids. In hardwoods, three major types of cells are found in this plant group: vase elements, fibers and ray cells, which constitute the radial parenchyma [44]. In general, the pinustracheids are longer in length than the eucalyptus fibers (Fig. 5).

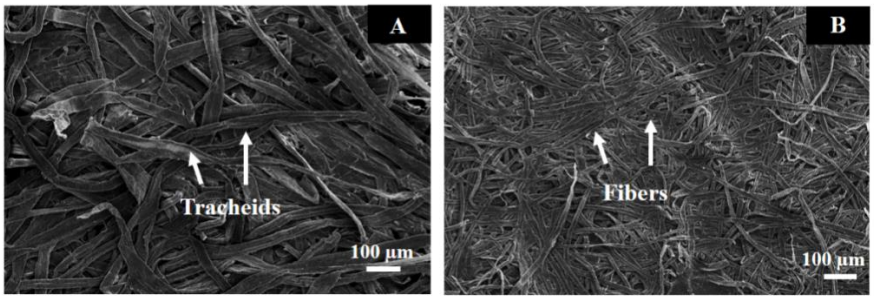

Fig. 5. Appearance of tracheids (A) and fibers (B) of bleached pulps.

The length of the cellulose fibers varies according to the wood source. The eucalyptus fibers are shorter (on average, 0.85 mm in length) than the pinustracheids (on average: 2.6 mm in length) [45,46]. Therefore, it is possible that the nanofibrils of pinus also presented greater length than those of eucalyptus.

The diffraction spectra showed the typical behavior of cellulosic materials. The crystalline index was higher for pinusnanofibrils (Fig. 6). Cellulose is a biopolymer that forms semicrystallinemicrofibrils comprised of organized crystalline regions connected by amorphous regions that occur in lower proportion [47]. The peaks that occurred in both diffractograms at 16.5˚ (correspondent to (1-10) and (110) planes) and 22.6˚ related to (200) plane are representative of the native cellulose I [48], with the crystalline peak occurring around 22.6˚ [49]. The values are consistent with some found in the literature. Viana[50] producing nanostructured cellulose films of blechedkraft pulp of pinus by mechanical griding, found crystalline index of 67.3% after 30 passes through the grinder. Lengowski[51] evaluated the crystalline index of cellulose nanofibrils from eucalyptus obtained by mechanical process at rotations of 1000 and 1500 rpm, and found lower values of crystallinity (around 64%). Increasing the crystalline character of the cellulose nanofibrils may alter their mechanical properties, increasing the tensile strength and elastic modulus and decreasing the elongation at break of the nanofibrils[52,53].

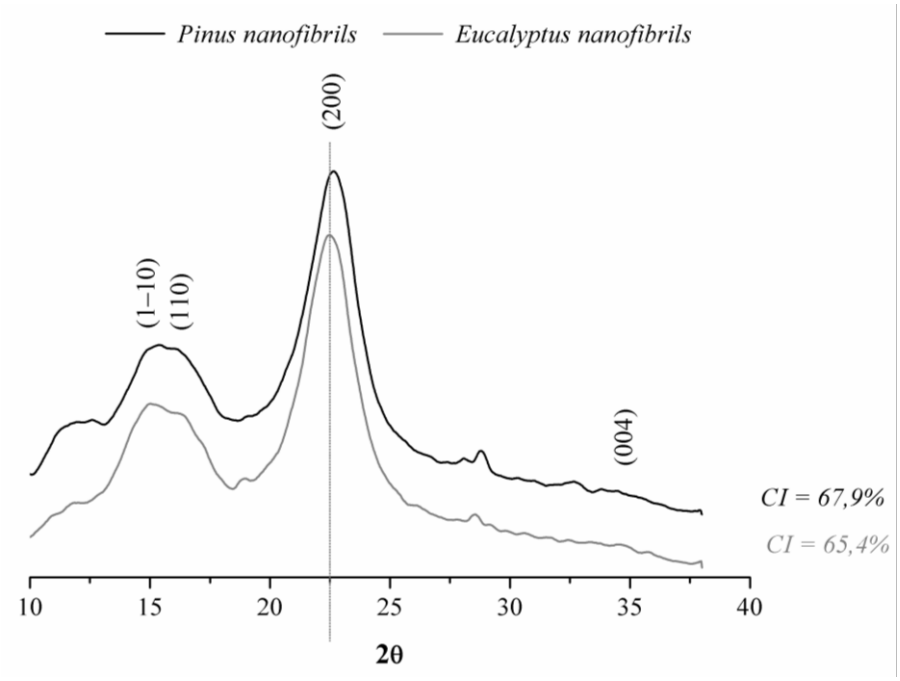

Fig. 6. Typical X-ray diffractogram and crystalline index (CI) of the eucalyptus and pinusnanofibrils.

3.3. Effect of corona treatment time on the performance ofnanofibril films

The nanofibrils of both wood genera were analyzed using ATR spectroscopy to observe the changes in their chemical composition after the discharges by corona treatment (Fig. 7 and Fig. 8). All the samples exhibited a broad absorption band in the region between 3500

and 3300 cm^{-1} corresponding to the free O–H stretching vibration of the OH groups in cellulose molecules [54]. The peak observed at 2916 cm^{-1} is associated with the stretching vibrations of C–H groups [55]. The spectral bands observed in the region around 1647–1638 $cm^{-1}$are attributed to the O–H bending of the adsorbed water [56].

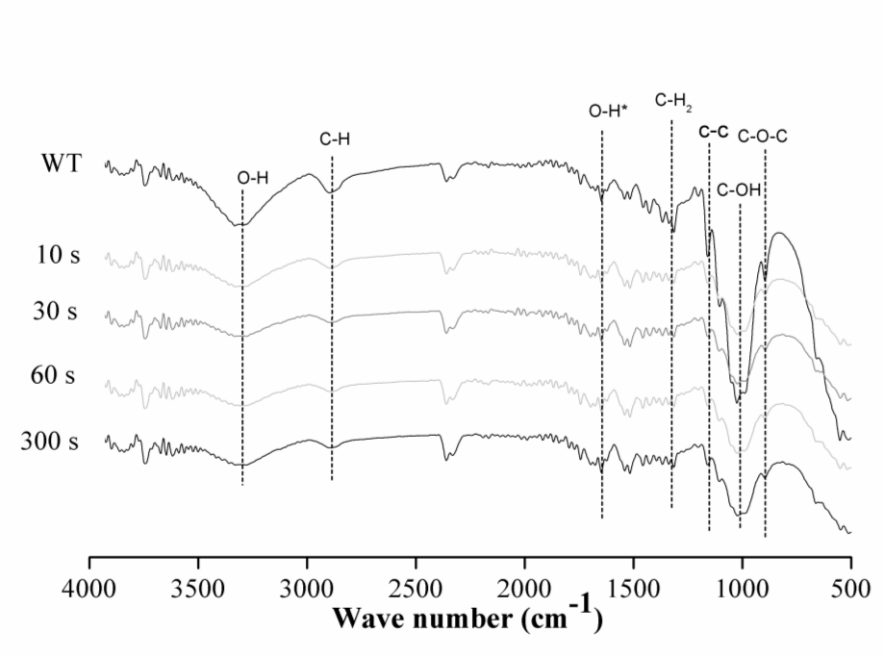

Fig. 7. Typical ATR spectra of the eucalyptus nanofibrils without treatment (WT) and of those submitted to different times (10, 30, 60 and 300 s) of corona treatment. * O–H bending of the adsorbed water.

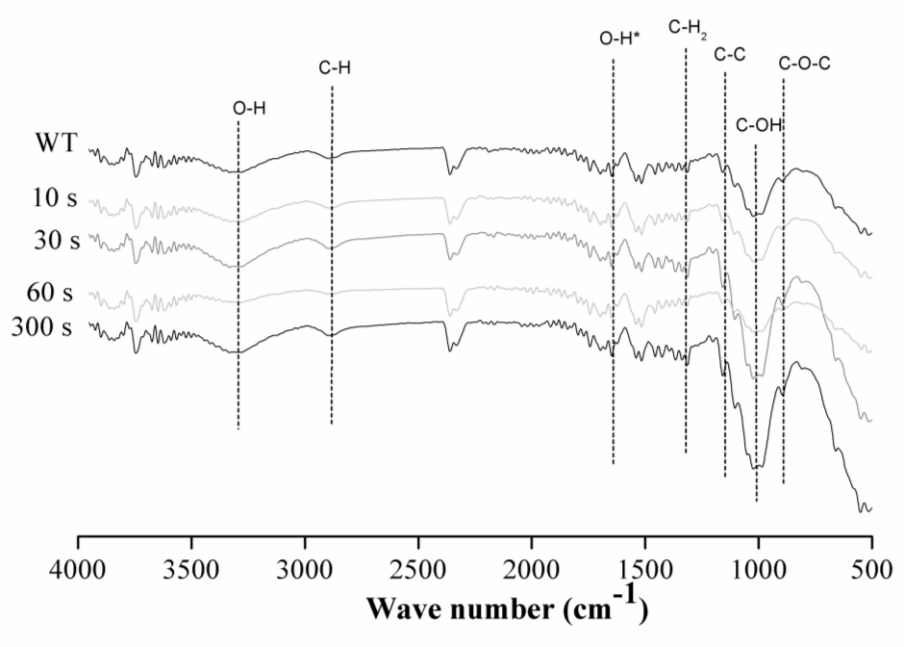

Fig. 8. Typical ATR spectra of the pinusnanofibrils without treatment (WT) and of those submitted to different times (10, 30, 60 and 300 s) of corona treatment. * O–H bending of the adsorbed water.

The interval between 1300 and 1400 cm^{-1} relates to CH_2 wagging in cellulose [57–59]. The region before 1300 cm^{-1} is related to C-O-C asymmetric stretching from glycosidic linkages, C-O stretching, C-O-C deformation [59–61].

At the wave number around 1317 cm^{-1}, a peak is formed in the spectra of the bleached fibers corresponding to the angular deformation of

the CH_2 cellulose bleached. Chemical groups occurring between 1170 and 1150 cm^{-1} and between 1050 and 103 cm^{-1}[49] become more intense in the spectra of bleached fibers for the same reason.

The bands at 1151 cm-^{1}are attributed to the C–C ring stretching [56]. The corona discharge resulted in the increase of the intensity of the bands at 1037 cm^{-1}, related to the hydrogen bonding (C-OH) in the cellulose skeleton [62,63]. In addition, this band became more intense due to the oxidation and rearrangement of the cellulose structure, being a strong evidence that the corona treatment alters the surface structure of the film [64]. The intensity of this peak increased with increases in the corona treatment time.

Therefore, corona discharge is expected to result in increased surface energy by oxidation, resulting in the formation of hydroxyl, carbonyl and other functional groups by the breakdown of C-C bonds and subsequent reaction with oxygen [65–67].

All the pulp samples of this study were fully bleached and contained almost zero lignin. Therefore, the region from 600 to 1500 cm^{-1} is primarily related to chemical groups of cellulose and hemicelluloses.

Characteristic bands of lignin, such as 1510, 1595, 1740 and 1770 cm^{-1}[61]could not be found in bleached pulp samples.

The average grammage values for the eucalyptus and pinusnanofibril films are in Table 2. Overall, pinusnanofibril films showed higher grammage than eucalyptus films.

Table 2. Average and standard deviation values of grammage of the nanofibril filmsfilms without treatment (WT) and after different times of corona discharge (10, 30, 60 and 300 s).

	Grammage ($g.m^{-2}$)	
Condition	**Eucalyptus**	**Pinus**
WT	15.92 ± 1.11*	21.49 ± 1.07
10 s	21.69 ± 2.47	21.19 ± 3.11
30 s	19.70 ± 0.90	27.36 ± 0.93
60 s	22.49 ± 1.18	20.50 ± 0.41
300 s	16.81 ± 2.95	22.79 ± 4.15

* Standard-deviation.

After evaporation of water of nanofibril suspension, the film is formed on the plate. Most films processed in this way are irregular in

grammage and thickness and still characterized by a heterogeneous fibrous structure [68]. Due to the smaller diameter of the pinusnanofibrils, a more compact and less porous structure is formed due to the larger surface area of the nanofibrils and the greater interaction between them.

It can be observed that the corona treatment promoted a considerable increase in the water vapor permeability with 30 s of the application of corona discharge, being of 13.1 g.mm/KPa.day.m² for the eucalyptus films and 14.2 g.mm/KPa.day.m² for the pinus films (Fig. 9).The corona discharge applied in atmospheric condition consists of positively charged ions, electrons, excited or metastable species of oxygen and nitrogen. The metastable oxygen species react with molecules in the atmosphere to generate ozone, a powerful oxidizing agent. The energies of the particles (1-20 eV) are sufficient to break C-C and C-H bonds (2.54 eV and 3.79 eV, respectively) and generate free radicals on the surface, which can react with atoms of oxygen and form polar groups[14].

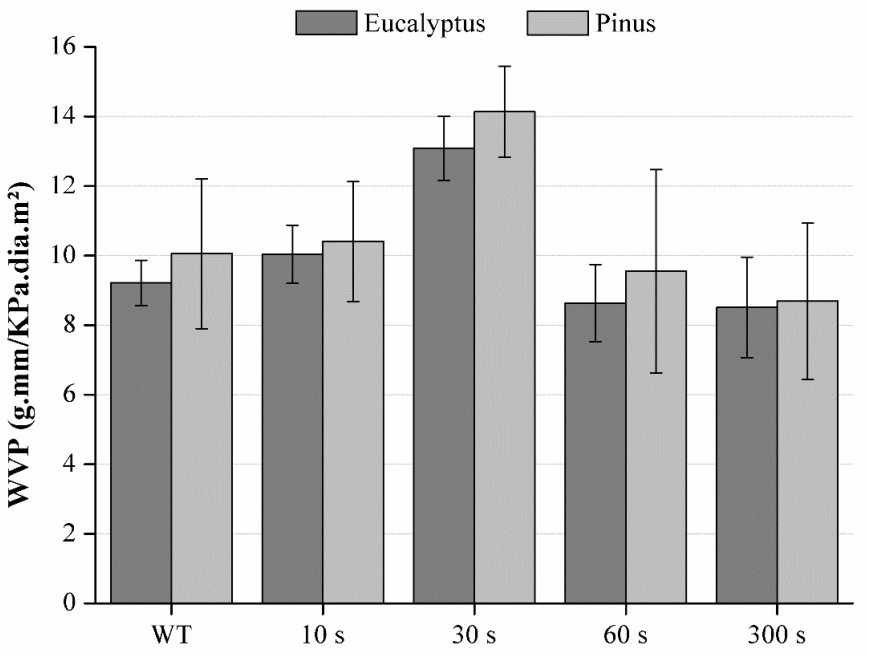

Fig. 9.Average and standard deviation values of water vapor permeability (WVP) of the eucalyptus and pinusnanofibrilwithout treatment (WT) and after different times of corona discharge (10, 30, 60 and 300 s).

Such surface modification may be advantageous for improving the printing on nanofibril films. Results obtained by Ryu, Wakida and Takagishi[69] indicated that corona discharge treatment was effective on improving wool fabric impression. Bergamasco[70], evaluating the physical properties in silk fabric after corona treatment, found that there was dyeing improvement.

In the present work it was found a reduction in the water vapor permeability values of the films for times higher than 30 s of corona discharge treatment. Chan [71]reported that longer treatment times promote increased roughness and crosslinking in some regions of a polymer surface providing an increase in the cohesive strength of the films, an than hindering the passage of water vapor.

The highest water absorption values (around 35%) for the films of both woodgenus were found for films treated with 30 s of corona discharge, corroborating with the water vapor permeability (Fig. 10 and Fig. 11).Corona typically converts the substrate surface from a nonpolar state to a polar state [10]and changes its topography causing an increase in roughness, which helps to facilitate the anchoring of paints and adhesives on the polymer surface[72].

When analyzing the effect of corona treatment on cotton fabric, Carvalho, Giordano and Campos[14]verified through tests of water absorption that no significant alterations on the absorption values could be observed after 24h of corona discharge in relation to the starting condition.

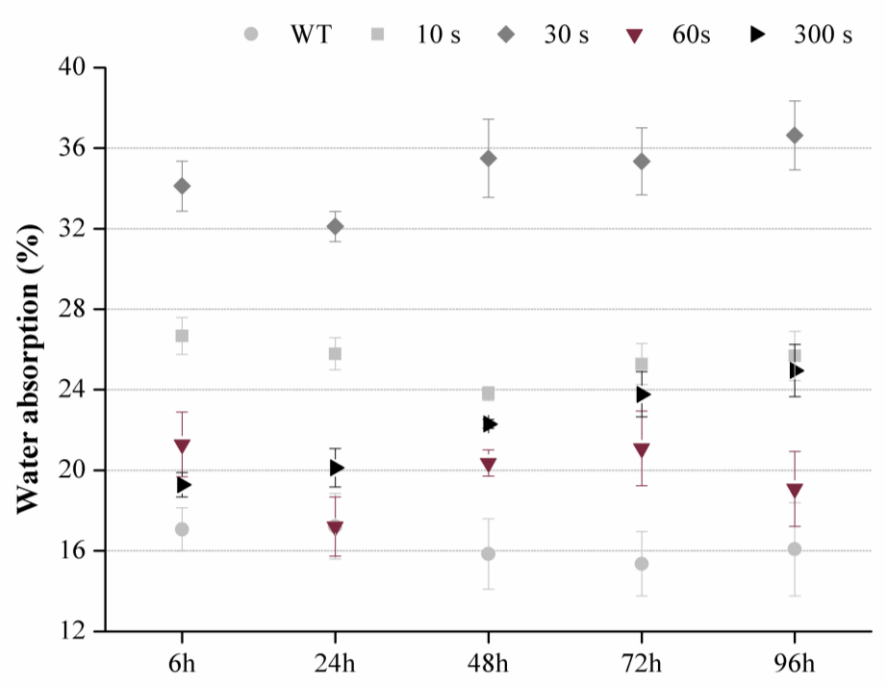

Fig. 10. Average and standard deviation values of water absorption of the eucalyptus films without treatment (WT) and after different times of corona discharge (10, 30, 60 and 300 s), in function of time after treatment (6, 24, 48, 72 and 96 h), in order to verify the length of the surface modification of the films.

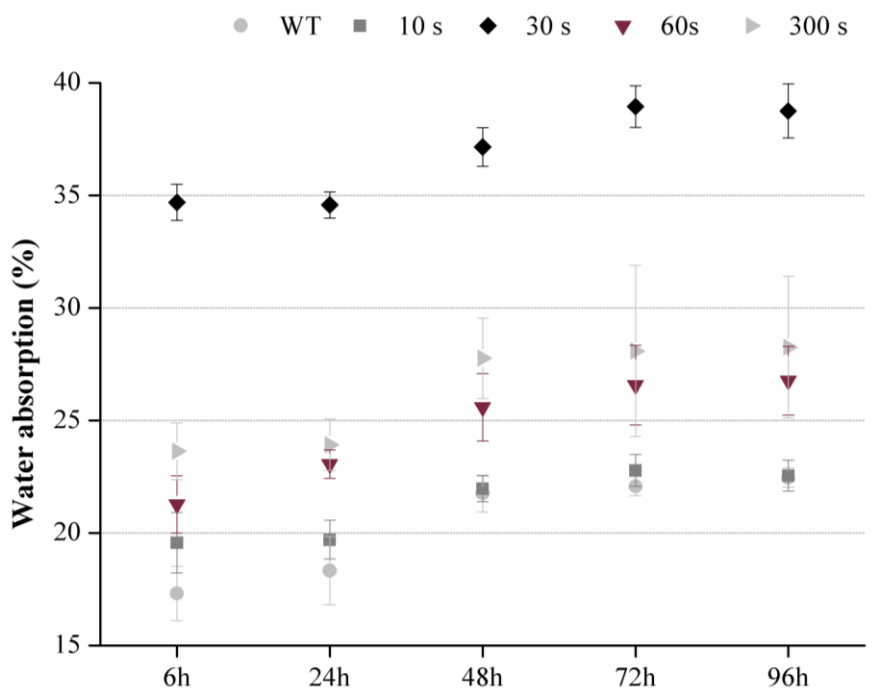

Fig. 11. Average and standard deviation values of water absorption of the pinus films without treatment (WT) and after different times of corona discharge (10, 30, 60 and 300 s), in function of time after treatment (6, 24, 48, 72 and 96 h), in order to verify the length of the surface modification of the films.

The nanofibril films were submitted to the tensile test as a function of the corona discharge time (10, 30, 60 and 300 s), from which the maximum tensile strength (σmáx) and the elastic modulus (E) were

obtained and divided the thegrammage (Gr) of the evaluated films (Fig. 12 and Fig. 13).

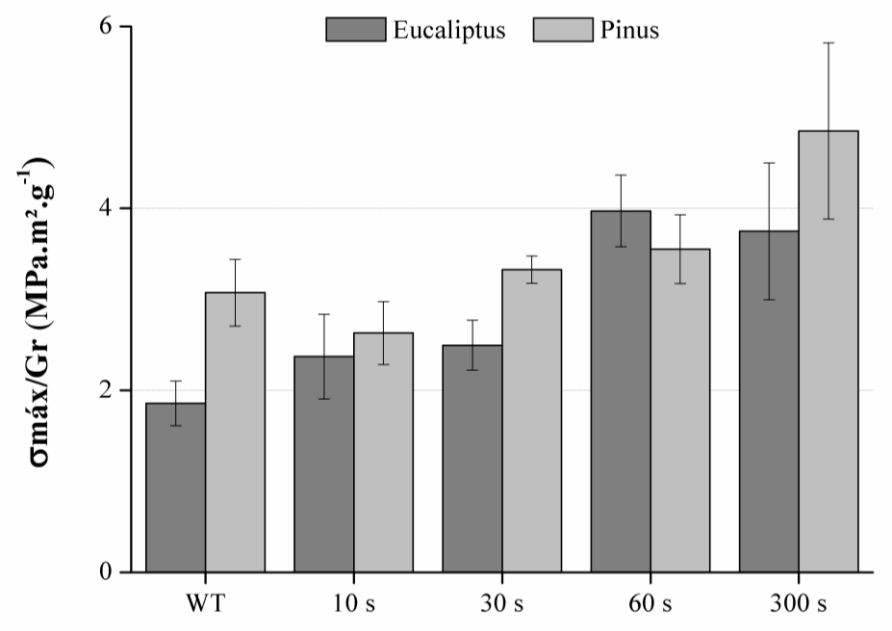

Fig. 12. Average and standard deviation values of maximum tensile strength (σmáx) divided by the grammage (Gr) of films, without treatment (WT) and submitted to different times (10, 30, 60 and 300 s) of corona treatment.

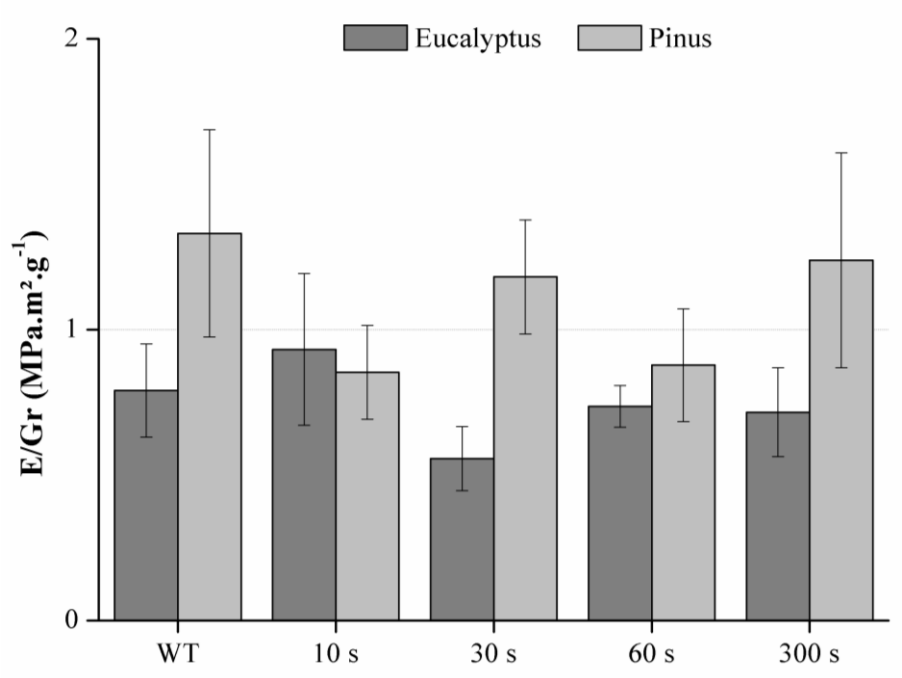

Fig. 13. Average and standard deviation values of elastic modulus (E) divided by grammage (Gr) of films without treatment (WT) and submitted to different times (10, 30, 60 and 300 s) of corona treatment.

It is observed that corona treatment does promote modifications in the mechanical properties of the films. In comparison with the WT films the σmáx increased by 102% for eucalyptus films and 60% for pinus films with 300 s of corona discharge application. Chan[71] reported that longer treatment times promote greater crosslinking in some regions of a polymer surface leading to the increase of cohesive strength between the

nanofibrils, contributing to increase mechanical strength of the films. Contrary, the E values were less influenced by corona discharges, leading to some diminution of E with the time of corona exposition (e.g. for 30 s for eucalyptus and 10 and 60 s for pinus).

As the pinusnanofibrils are probably longer than eucalyptus nanofibrils due to longer tracheids in comparison to eucalyptus fibers, they may present a larger aspect ratio, which is directly related to higher tensile strength [73].

3.4. Duration of the corona treatment

The contact angle (°) of water with the surface of the nanofibril filmswas evaluated as a function of the time elapsed after the corona discharge (Fig. 14 and Fig. 15). Nanofibril films treated during 30 s by corona discharge were selected in this evaluation, because this time of exposition to corona proved to be the most effective for increasing the hydrophilicity of the films (as reported in Fig. 9, Fig. 10 and Fig 11). It is observed that the films without treatment (WT) presented contact angle of 70 ± 2° for eucalyptus and 58 ± 5° for pinus. These values drastically reduce when

the contact angle was measured immediately after the application of the corona discharge (0h).

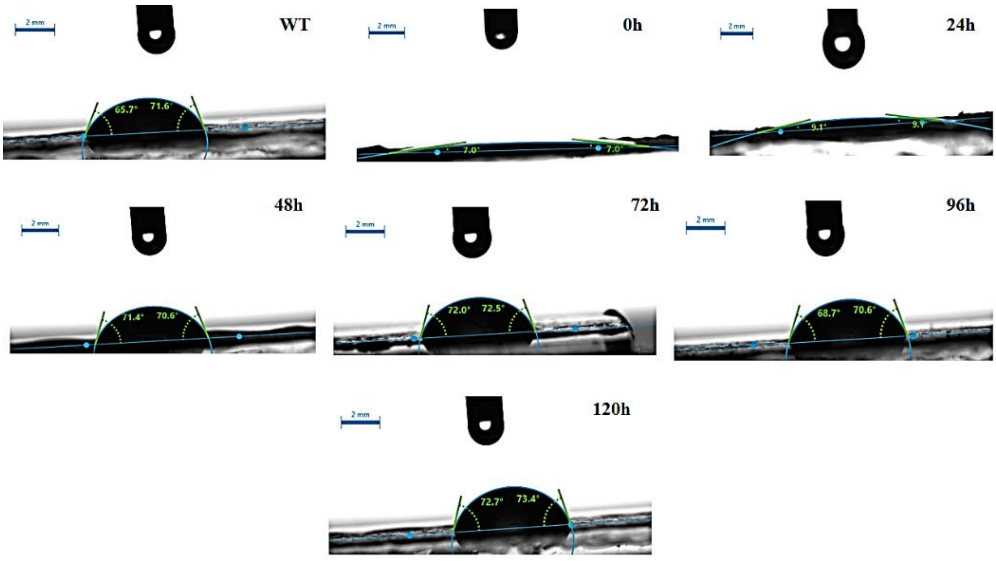

Fig. 14. Contact angle of water with the eucalyptus nanofibril film substrate without treatment (WT) and with 30 s of corona discharge, for evaluation of the length of the treatment modifications along the time (0, 24, 48, 72, 96 and 120 h after discharges).

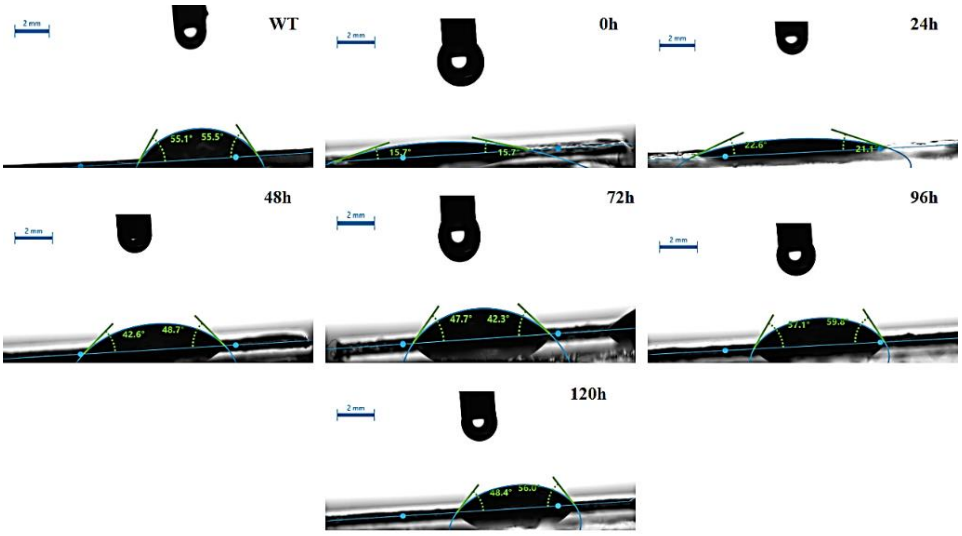

Fig. 15. Contact angle of water with the pinusnanofibril film substrate without treatment (WT) and with 30 s of corona discharge, for evaluation of the length of the treatment modifications along the time (0, 24, 48, 72, 96 and 120 h after discharges).

Nanofibril films treated with 30 s of corona discharge were exposed to laboratory atmosphere for different times, and it was observed that even after 24 h, the films still presents their surfaces modified by the treatment. Otherwise 48 h after corona application, the surface changes were completely lost for eucalyptus films and remarkably reduced for

pinus films, since the contact angles values became similar to values of the films without treatment.

The contact angles after 0 h and 24 h were lower for eucalyptus films. The previously mentioned roughness of pinus films possibly provide resistance for the sliding of water droplets [74].

The values of the free surface energy of the films, and its dispersive and polar components as a function of time after the corona discharge is presented in Table 3. It should be noted that there was a large increase in the free surface energy of the films immediately after corona treatment (0 h) was applied. For eucalyptus films, surface energy increased by 37% and for pine films this increase was 25%.

Table 3. Free surface energy of the films and their polar components and dispersion as a function of time after the application of corona discharge.

Time	**Surface free energy[mN.m^{-1}]**		**Disperse [mN.m^{-1}]**		**Polar [mN.m^{-1}]**	
	Eucalyptus	**Pinus**	**Eucalyptus**	**Pinus**	**Eucalyptus**	**Pinus**
WT	59.67 ± 1.41*	55.29 ± 1.21	39.91 ± 0.70	39.05 ± 0.61	19.76 ± 1.24	16.24 ± 0.67
0h	78.98 ± 0.35	69.22 ±4.71	47.18 ± 0.68	40.52 ± 1.15	31.59 ± 0.59	28.70 ± 5.85
48h	58.89 ± 1.08	54.89 ± 1.18	37.65 ± 0.63	37.04 ± 1.07	21.24 ± 1.15	17.85 ± 0.45

* Standard-deviation; WT – films without treatment

The oxygen molecules in the corona discharge films are free to bond to the ends of the molecules in the substrate to be treated, resulting in an increase in surface tension[10].In the work conducted by Cernak, Sebo and Skalny[75], carbon fibers were treated with corona discharge, with a voltage between 2 and 3 kV, and current intensity between 15 and 80 μA. The results showed that the process increases the fiber surface free energy up to 20%.

After 48 hours of application of the corona discharge, the value of the surface energy is similar to the value of the superficial energy of the films without treatment, which corroborates to the fact that the corona treatment effect lasts no longer than 24 hours.This can be attributed to secondary reactions with species present in atmospheric air, and contaminants that can be gradually adsorbed onto the surface of the film[72].

4. Conclusions

Aiming the use ofnanofibril films for printing, a higher surface energy is desirable. Our findingsshowed that corona treatment performed for 30 scaused maximum water vapor permeability and maximum water

absorption values for films of both wood genus studied here (eucalyptus and pinus), what may optimizes the ink penetration.

Corona discharge caused increase of the tensile strength with increase of discharge time, while caused an apparent diminution of the elastic modulus. Tests showed that the length or duration of the corona treatment seems to be around 24 h. The effect of the corona treatment was similar for films of eucalyptus and pinusnanofibrils, and films from pine pulp seems to present higher performance.

Further studies should be carried out in order to observe the effect of the combination of different application distances and times of application of the corona discharge on the properties of thenanofibril films. The present study contributed with information about surface modification of cellulose nanofibrils films with corona discharge, and further progress of this approach could improve the performance of cellulose based materials several applications.

5. Acknowledgments

The authors appreciate the financial support of the Minas Gerais Research Funding Foundation (FAPEMIG), National Council for

Scientific and Technological Development (CNPq) and Coordination for the Improvement of Higher Education Personnel (CAPES).

5. References

[1] M.A. Martins, L.H.C. Mattoso, J.D.C. Pessoa, Thermogravimetric evaluation of açaí fruit (Euterpeoleracea Mart.) agro industry waste, Rev. Bras. Frutic. 31 (2009) 1150–1157.

[2] L. Bufalino, A.R. de Sena Neto, G.H.D. Tonoli, A. de Souza Fonseca, T.G. Costa, J.M. Marconcini, J.L. Colodette, C.R.G. Labory, L.M. Mendes, How the chemical nature of Brazilian hardwoods affects nanofibrillation of cellulose fibers and film optical quality, Cellulose. 22 (2015) 3657–3672.

[3] H.P.S. Abdul Khalil, Y. Davoudpour, M.N. Islam, A. Mustapha, K. Sudesh, R. Dungani, M. Jawaid, Production and modification of nanofibrillated cellulose using various mechanical processes: A review, Carbohydr. Polym. 99 (2014) 649–665.

[4] F. Jiang, Y.-L. Hsieh, Chemically and mechanically isolated nanocellulose and their self-assembled structures, Carbohydr. Polym. 95 (2013) 32–40.

[5] D. Klemm, F. Kramer, S. Moritz, T. Lindström, M. Ankerfors, D. Gray, A. Dorris, Nanocelluloses: A New Family of Nature-Based Materials, Angew. Chemie Int. Ed. 50 (2011) 5438–5466.

[6] Y. Chen, B. Geng, J. Ru, C. Tong, H. Liu, J. Chen, Comparative characteristics of TEMPO-oxidized cellulose nanofibers and resulting nanopapers from bamboo, softwood, and hardwood pulps, Cellulose. 24 (2017) 4831–4844.

[7] L. Hu, G. Zheng, J. Yao, N. Liu, B. Weil, M. Eskilsson, E. Karabulut, Z. Ruan, S. Fan, J.T. Bloking, M.D. McGehee, L. Wågberg, Y. Cui, Transparent and conductive paper from nanocellulose fibers, Energy Environ. Sci. 6 (2013) 513–518.

[8] H. Sehaqui, N.E. Mushi, S. Morimune, M. Salajkova, T. Nishino, L.A. Berglund, Cellulose Nanofiber Orientation in Nanopaper and Nanocomposites by Cold Drawing, ACS Appl. Mater. Interfaces. 4 (2012) 1043–1049.

[9] M. Kurek, F. Debeaufort, Surface modification of packaging films by coatings with bioactive compounds and biopolymers, in: M. Kontominas (Ed.), Bioact. Food Packag. Strateg. Qual. Saf., 2015: p. 474.

[10] R.A. Wolf, Plastic surface modification : surface treatment and adhesion, Carl Hanser, 2015.

[11] M.N. Belgacem, P. Bataille, S. Sapieha, Effect of corona modification on the mechanical properties of polypropylene/cellulose composites, J. Appl. Polym. Sci. 53 (1994) 379–385.

[12] J. Gassan, V.S. Gutowski, Efects of corona discharge and UV treatment on the properties of jute-fbre epoxy composites, Compos. Sci. Technol. 60 (2000) 2857–2863.

[13] R.G. de A. Mesquita, A.A. da S. César, R.F. Mendes, L.M. Mendes, J.M. Marconcini, G. Glenn, G.H.D. Tonoli, Polyester Composites Reinforced with Corona-Treated Fibers from Pine, Eucalyptus and Sugarcane Bagasse, J. Polym. Environ. 25 (2017) 800–811.

[14] J.G.; Carvalho, J.B. Giordano, J.S.C. Campos, Medidas quantitativas de absorção de água em tecidos de algodão e poliéster antes e após trtamento corona., Quím Têxtil. 108 (2012) 58–67.

[15] NBR 7989 “Pasta celulósica e madeira: determinação de lignina insolúvel em ácido”, Associação Brasileira De Normas Técnicas, ABNT 2010, Rio de Janeiro, BR.

[16] B.L. Browning, The composition and chemical reactions of wood, in: Chem. Wood, American Association for the Advancement of Science, 1963: pp. 1564–1564.

[17] J.F. Kennedy, G.O. Phillips, P.A. Williams, Wood and cellulosics : industrial utilization, biotechnology, structure, and properties, E. Horwood, 1987.

[18] Q.Q. Wang, J.Y. Zhu, R. Gleisner, T.A. Kuster, U. Baxa, S.E. McNeil, Morphological development of cellulose fibrils of a bleached eucalyptus pulp by mechanical fibrillation, Cellulose. 19 (2012).

[19] M.V. Scatolino, L. Bufalino, L.M. Mendes, M. Guimarães Júnior, G.H.D. Tonoli, Impact of nanofibrillation degree of eucalyptus and Amazonian hardwood sawdust on physical properties of cellulose nanofibril films, Wood Sci. Technol. 51 (2017) 1095–1115.

[20] L. Segal, J.J. Creely, A.E. Martin, C.M. Conrad, An Empirical Method for Estimating the Degree of Crystallinity of Native Cellulose Using the X-Ray Diffractometer, Text. Res. J. 29 (1959) 786–794.

[21] E 96-00 "Standard Test Methods for Water Vapor Transmission of Materials", American Society For Testing And Materials Standards, ASTM 2016, West Conshohocken, PA.

[22] M. Guimarães, V.R. Botaro, K.M. Novack, F. Gomes Teixeira, G. Henrique, D. Tonoli, Starch/PVA-based nanocomposites reinforced with bamboo nanofibrils, Ind. Crops Prod. 70 (2015) 72–83.

[23] O. Tetens, Uber einige meteorologische begriffe, Z. Geophys. 6 (1930) 297–309.

[24] A.L. da Róz, Preparação e caracterização de amidos termoplásticos, Biblioteca Digital de Teses e Dissertações da Universidade de São Paulo, 2004.

[25] E 104-02 "Standard Practice for Maintaining Constant Relative Humidity by Means of Aqueous Solutions" American Society For Testing And Materials Standards, ASTM 2012, West Conshohocken, PA.

[26] D 882-12 “Standard Test Method for Tensile Properties of Thin Plastic Sheeting”, American Society For Testing And Materials, ASTM 2012, West Conshohocken, PA, 2012.

[27] E. Sjöström, Wood chemistry : fundamentals and applications, 1981.

[28] W. Li, R. Wang, S. Liu, NANOCRYSTALLINE CELLULOSE PREPARED FROM SOFTWOOD KRAFT PULP VIA ULTRASONIC-ASSISTED ACID HYDROLYSIS, BioResources. 6 (2011) 4271–4281.

[29] S. Iwamoto, a. N. Nakagaito, H. Yano, M. Nogi, Optically transparent composites reinforced with plant fiber-based nanofibers, Appl. Phys. A Mater. Sci. Process. 81 (2005) 1109–1112. doi:10.1007/s00339-005-3316-z.

[30] S. Janardhnan, M. Sain, Bio-Treatment of Natural Fibers in Isolation of Cellulose Nanofibres: Impact of Pre-Refining of Fibers on Bio-Treatment Efficiency and Nanofiber Yield, J. Polym. Environ. 19 (2011) 615–621. doi:10.1007/s10924-011-0312-6.

[31] K.L. Spence, R.A. Venditti, O.J. Rojas, Y. Habibi, J.J. Pawlak, A comparative study of energy consumption and physical properties of microfibrillated cellulose produced by different processing methods, Cellulose. 18 (2011) 1097–1111.

[32] J. Vartiainen, T. Pöhler, K. Sirola, L. Pylkkänen, H. Alenius, J. Hokkinen, U. Tapper, P. Lahtinen, A. Kapanen, K. Putkisto, P. Hiekkataipale, P. Eronen, J. Ruokolainen, A. Laukkanen, Health and environmental safety aspects of friction grinding and spray drying of microfibrillated cellulose, Cellulose. 18 (2011) 775–786.

[33] S. Iwamoto, K. Abe, H. Yano, The Effect of Hemicelluloses on Wood Pulp Nanofibrillation and Nanofiber Network Characteristics, Biomacromolecules. 9 (2008) 1022–1026. doi:10.1021/bm701157n.

[34] J.I. Morán, V.A. Alvarez, V.P. Cyras, A. Vázquez, Extraction of cellulose and preparation of nanocellulose from sisal fibers, Cellulose. 15 (2008) 149–159.

[35] T. Virtanen, S.L. Maunu, T. Tamminen, B. Hortling, T. Liitiä, Changes in fiber ultrastructure during various kraft pulping conditions evaluated by 13 C CPMAS NMR spectroscopy, (2007).

[36] H. Zhang, M. Tong, Influence of hemicelluloses on the structure and properties of Lyocell fibers, Polym. Eng. Sci. 47 (2007) 702–706.

[37] J.L. COLODETTE, J.L. GOMIDE, R. GIRARD, A.-S. JAASKELAINEN, D.S. ARGYROPOULOS, Influence of pulping conditions on eucalyptus kraft pulp yield, quality, and bleachability, TAPPI J. 1 (2002) 20.

[38] O. Nechyporchuk, M.N. Belgacem, J. Bras, Production of cellulose nanofibrils: A review of recent advances, Ind. Crop. Prod. 93 (2016) 2–25.

[39] A.N. Nakagaito, H. Yano, Novel high-strength biocomposites based on microfibrillated cellulose having nano-order-unit web-like network structure, Appl. Phys. A. 80 (2005) 155–159.

[40] A.G. Barneto, C. Vila, J. Ariza, Eucalyptus kraft pulp production: Thermogravimetry monitoring, Thermochim. Acta. 520 (2011) 110–120.

[41] T.E.S. Segura, Avaliação das madeiras de Eucalyptus grandis x Eucalyptus urophylla e Acacia mearnsii para a produção de celulose kraft pelos processos convencional e Lo-Solids®, Biblioteca Digital de Teses e Dissertações da Universidade de São Paulo, 2011.

[42] R.S.P. Coutts, A review of Australian research into natural fibre cement composites, Cem. Concr. Compos. 27 (2005) 518–526.

[43] I. Siró, D. Plackett, Microfibrillated cellulose and new nanocomposite materials: A review, Cellulose. 17 (2010) 459–494.

[44] R.M. Rowell, Handbook of wood chemistry and wood composites, Taylor & Francis, 2012.

[45] L. de C. Fidale, Biopolímeros modificados: aspectos de derivatização de celulose sob condições homogêneas de reação, Biblioteca Digital de Teses e Dissertações da Universidade de São Paulo, 2010.

[46] J.E. Levlin, L. Söderjhelm, Pulp and paper testing, Fapet Oy, 1999.

[47] M. Ioelovich, A. Leykin, Structural investigations of various cotton fibers and cotton celluloses, BioResources. 3 (2008) 170–177.

[48] Y. Nishiyama, J. Sugiyama, H. Chanzy, P. Langan, Crystal Structure and Hydrogen Bonding System in Cellulose Iα from Synchrotron X-ray and Neutron Fiber Diffraction, J. Am. Chem. Soc. 125 (2003) 14300–14306.

[49] A.C. Corrêa, E. de Morais Teixeira, L.A. Pessan, L.H.C. Mattoso, Cellulose nanofibers from curaua fibers, Cellulose. 17 (2010) 1183–1192.

[50] L.C. Viana, Desenvolvimento de filmes celulósicos nanoestruturados a partis da polpa Kraft de *Pinus* sp., (2013).

[51] E.C. Lengowski, Caracterização e predição da cristalinidade de celulose através de espectroscopia no infravermelho e análise multivariada, Universidade Federal Do Paraná, 2012.

[52] S. Iwamoto, A.N. Nakagaito, H. Yano, Nano-fibrillation of pulp fibers for the processing of transparent nanocomposites, Appl. Phys. A. 89 (2007) 461–466.

[53] K. Uetani, H. Yano, Nanofibrillation of Wood Pulp Using a High-Speed Blender, Biomacromolecules. 12 (2011) 348–353.

[54] C.J. Chirayil, J. Joy, L. Mathew, M. Mozetic, J. Koetz, S. Thomas, Isolation and characterization of cellulose nanofibrils from Helicteres isora plant, Ind. Crops Prod. 59 (2014) 27–34.

[55] B. Deepa, E. Abraham, N. Cordeiro, M. Mozetic, A.P. Mathew, K. Oksman, M. Faria, S. Thomas, L.A. Pothan, Utilization of various lignocellulosic biomass for the production of nanocellulose: a comparative study, Cellulose. 22 (2015) 1075–1090.

[56] A. Mandal, D. Chakrabarty, Isolation of nanocellulose from waste sugarcane bagasse (SCB) and its characterization, Carbohydr. Polym. 86 (2011) 1291–1299.

[57] M. Åkerholm, B. Hinterstoisser, L. Salmén, Characterization of the crystalline structure of cellulose using static and dynamic FT-IR spectroscopy, Carbohydr. Res. 339 (2004) 569–578.

[58] M. Åkerholm, L. Salmén, Interactions between wood polymers studied by dynamic FT-IR spectroscopy, Polymer (Guildf). 42 (2001) 963–969.

[59] F. Carrillo, X. Colom, J.. Suñol, J. Saurina, Structural FTIR analysis and thermal characterisation of lyocell and viscose-type fibres, Eur. Polym. J. 40 (2004) 2229–2234.

[60] H. Chen, C. Ferrari, M. Angiuli, J. Yao, C. Raspi, E. Bramanti, Qualitative and quantitative analysis of wood samples by Fourier transform infrared spectroscopy and multivariate analysis, Carbohydr. Polym. 82 (2010) 772–778.

[61] C.-M. Popescu, M.-C. Popescu, G. Singurel, C. Vasile, D.S. Argyropoulos, S. Willfor, Spectral Characterization of Eucalyptus Wood, Appl. Spectrosc. 61 (2007) 1168–1177.

[62] J.A.O. Barros, F. de A. Silva, R.D. Toledo Filho, Experimental and numerical research on the potentialities of layered reinforcement configuration of continuous sisal fibers for thin mortar panels, Constr. Build. Mater. 102 (2016) 792–801.

[63] A. Elkhaoulani, F.Z. Arrakhiz, K. Benmoussa, R. Bouhfid, A. Qaiss, Mechanical and thermal properties of polymer composite based on natural fibers: Moroccan hemp fibers/polypropylene, Mater. Des. 49 (2013) 203–208.

[64] M.A.S. Spinacé, C.S. Lambert, K.K.G. Fermoselli, M.-A. De Paoli, Characterization of lignocellulosic curaua fibres, Carbohydr. Polym. 77 (2009) 47–53.

[65] L. Klarhöfer, W. Viöl, W. Maus-Friedrichs, Electron spectroscopy on plasma treated lignin and cellulose, Holzforschung. 64 (2010).

[66] C. Relvas, G. Castro, S. Rana, R. Fangueiro, Characterization of Physical, Mechanical and Chemical Properties of Quiscal Fibres: The Influence of Atmospheric DBD Plasma Treatment, Plasma Chem. Plasma Process. 35 (2015) 863–878.

[67] A. Temiz, S. Akbas, I. Aydin, C. Demirkir, The effect of plasma treatment on mechanical properties, surface roughness and durability of plywood treated with copper-based wood preservatives, Wood Sci. Technol. 50 (2016) 179–191.

[68] O.B.G. Assis, V.L. Silva, Caracterização estrutural e da capacidade de absorção de água em filmes finos de quitosana processados em diversas concentrações, Polímeros. 13 (2003) 223–228.

[69] J. Ryu, T. Wakida, T. Takagishi, Effect of Corona Discharge on the Surface of Wool and Its Application to Printing, Text. Res. J. 61 (1991) 595–601..

[70] D.A. Bergamasco, Caracterização de propriedades físicas em tecido de seda após tratamento pelos métodos de degomagem e por descarga corona, Universidade Estadual De CampinaS, 2015.

[71] C.M. Chan, Polymer surface modification and characterization, Hanser, 1993.

[72] N. Sellin, Analise da superficie de polimeros pos-tratamento corona, [s.n.], 2002.

[73] M.L. Menegazzo, Características Morfológicas De Celuloses Branqueadas De Pinus E Eucalyptus Em Analisador Óptico Automático De Fibras, Faculdade de Ciências Agronômicas da UNESP – Câmpus de Botucatu, 2012.

[74] M. Miwa, A. Nakajima, A. Fujishima, K. Hashimoto, T. Watanabe, Effects of the Surface Roughness on Sliding Angles of Water Droplets on Superhydrophobic Surfaces, Langmuir. 16 (2000) 5754–5760.

[75] M. Cernak, P. Sebo, J. Skalny, The Treatment Of Carbon-Fibers Surface In Positive Corona Discharge, Acta Phys. Slovaca. 35 (1985) 23–26